Energy retrofitting of the Olimpia motorway tunnel

Tunnelling and Underground Space Technology 173 (2026) 107595

Contents lists available at ScienceDirect

Tunnelling and Underground Space Technology incorporating Trenchless Technology Research

journal homepage: www.elsevier.com/locate/tust

Energy retrofitting of the Olimpia motorway tunnel

S. De Feudis *, A. Insana, M. Barla

Department of Structural, Geotechnical and Building Engineering, Politecnico di Torino, Turin, Italy

A B S T R A C T

Nowadays, the increasing deterioration of existing infrastructure requires refurbishment to guarantee service continuation in safe conditions. However, this may represent a valuable opportunity to renovate the existing heritage of infrastructures not only from a structural but also from a sustainable viewpoint. The paper illustrates the first-ever documented case of an existing tunnel section systematically converted into an energy geostructure during rehabilitation works. The geothermal piping arranged in the tunnel lining is connected using pre-insulated collectors to other heat exchanger pipes embedded in the motorway pavement. Such a geothermal system is now being tested against anti-icing and solar-collecting purposes in winter and summer, respectively. A comprehensive overview of the additional installation stages needed to energy-retrofit the existing tunnel is provided, along with a description of the adopted methodology. Then, the pressure and thermal response testing needed to verify the integrity and functionality of the system are described. Finally, the paper discloses the outcomes of the solar-collecting and anti-icing test campaigns.

1. Introduction

Tunnels are resilient geotechnical structures that generally remain serviceable for much longer than their designed serviceability, thus increasing the number of existing tunnels still in operation with an average service life of more than 50 years (Pigorini, 2020). Suffice it to think that, for instance, Swiss, Austrian and British railway concessionaires oversee, respectively, around 76.8 km, 250.0 km and 335.0 km, many of which are centenary or even older (Grossauer et al., 2017; Seywald et al., 2017; Atkinson et al., 2021).

Tunnelling in Italy has always played a pivotal role in the growth of the national railway and motorway networks because of the complex orography shaped by the Alps in the North and the Apennines throughout the whole peninsula. Indeed, *Rete Ferroviaria Italiana S.p.A.* runs a network of 24,500.0 km, with roughly 1460 railway tunnels, which correspond to an overall length of 1,480.0 km. Two-thirds of the existing track network was built before 1930. Hence, it stands to reason that 800.0 km of them are ancient tunnels (Fava et al., 2019). Similarly, as depicted in Fig. 1, *Autostrade per l'Italia S.p.A.*, a major motorway concessionaire, oversees more than 2,900.0 km of motorways, with about 365.0 km running through 595 tunnels. Around 60% of them were built during the booming Italian economy (1960–1980), thus lacking any waterproofing system (Mazzola et al., 2023) and approaching or even exceeding 50 years of service (Panebianco, 2023).

Fig. 1 also emphasises another paramount aspect. Taking *Autostrade per l'Italia S.p.A.* as an example, it seems evident that the development of the motorway network has considerably slowed down since the early 2000s. This is a symptom that attention is edging toward the management and refurbishment of the existing network rather than expansion and development. This applies to most well-established motorway and railway network overseers. The rationale behind such a shift in perspective has just been hinted at above and lies in the ageing of existing infrastructures that is increasingly becoming a risk to owners, concessionaires and customers in terms of investment and property value protection, revenue growth and infrastructure safety and efficiency, respectively.

Such a significant shift towards the refurbishment of existing tunnels rather than the construction of new infrastructures may pave the way for developing sustainable solutions for instrumenting existing tunnels for geothermal energy exploitation, thus converting them into energy geostructures. These are ground-embedded structures which accomplish the twofold aim of structural support and heat exchange (Brandl, 2006; Laloui & Di Donna, 2013). Indeed, heat exchanger pipes are embedded into structural elements and convey a heat carrier fluid, commonly water or water-glycol mixtures, thus transforming geotechnical structures into low-enthalpy geothermal systems. As such, these allow heat extraction and injection during winter and summer, respectively.

Throughout the years, extensive research has been carried out on energy tunnels about the implementation aspects (Unterberger et al., 2004; Adam & Markiewicz, 2009; Franzius & Pralle, 2011; Barla et al., 2019), the thermo-mechanical implications induced by heat exchange on the lining (Nicholson et al., 2014; Insana et al., 2020; Ma et al., 2022; Rotta Loria et al., 2022) and the amount of extractable and injectable heat as a function of the hydrogeological settings (Di Donna & Barla,

* Corresponding author.
E-mail address: simone.defeudis@polito.it (S. De Feudis).

https://doi.org/10.1016/j.tust.2026.107595
Received 10 November 2025; Received in revised form 18 February 2026; Accepted 1 March 2026

2016; Bidarmaghz & Narsilio, 2018; Insana & Barla, 2020; Ma et al., 2021; Alvi et al., 2022), the aerothermal conditions of the underground environment (Buhmann et al., 2016; Peltier et al., 2019; Ma et al., 2021; Dornberger et al., 2022; De Feudis et al., 2024) and the design and operational features (Cousin et al., 2019; Insana & Barla, 2020; Ogunleye et al., 2021). However, some technical and non-technical key issues remain to be addressed to foster their large-scale implementation. For instance, from the usage viewpoint, the necessity to integrate these systems with district heating networks and envisage resilient backup systems arises distinctly (Meibodi & Loveridge, 2022; Barla & Insana, 2023). Also, from the legal point of view, the clear distinction between the owners of the heat exchanger facilities and the exploitable energy is paramount, as well as the definition of the customers that can benefit from the system (Barla et al., 2021; Rotta Loria, 2021).

Furthermore, looking at the energy tunnel full-scale implementation realised so far (Adam & Markiewicz, 2009; Frodl et al., 2010; Franzius & Pralle, 2011; Zhang et al., 2014; Buhmann et al., 2016; Barla et al., 2019; Guan & Cheng, 2023; Kong et al., 2023), these have only dealt with new tunnelling projects. The sole exception is the Seocheon abandoned tunnel experimental site, where, however, energy textile modules were tested to instrument newly built tunnels (Lee et al., 2012, 2016,). From this overview, it seems evident that, until very recently, the opportunity to thermally activate existing tunnels has not been investigated.

Recently, De Feudis et al. (2024) proposed several energy retrofitting solutions to instrument existing tunnels for heat exchange, taking advantage of refurbishment strategies, and this paper illustrates the first-ever existing tunnel converted into an energy geostructure during rehabilitation works, by employing one of these energy retrofitting solutions. The study aims to demonstrate the feasibility of the energy retrofitting approach and propose a novel application to enhance road safety. Indeed, to achieve a seasonal operational cycle, the energy tunnel is connected to another piping embedded within a motorway pavement stretch outside the portal. The geothermal anti-icing solar-collecting system thus realised has the double aim of avoiding hoar frost formation during winter and catching solar thermal energy to be stored in the ground during summer.

A comprehensive overview of the additional installation stages needed to achieve the energy retrofitting of the existing tunnel will be provided, along with a brief description of the adopted methodology. Then, the pressure and thermal response testing needed to verify the integrity and functionality of the system are described, and the results are interpreted. Finally, the outcomes of a 16.5-day solar-collecting test and a 17.0-day anti-icing test performed during, respectively, summer and winter operations are shown and discussed.

2. Rehabilitation plan for the Olimpia tunnel

The Olimpia tunnel is a twin-tube, three-lane motorway tunnel located on the A26 motorway stretch between Casale Monferrato and Alessandria in North-West Italy. The 891.0 m long tunnel was excavated mainly through the heading-and-bench technique (814.0 m). The remaining portion (77.0 m) was realised with the cut-and-cover method due to the small cover at the entrances. The maximum overburden of about 40.0 m is reached in the central section of the Olimpia tunnel.

The construction works, which were completed around the '70s, envisaged steel lattice girders to support the top-heading excavation. Thick horizontal beams were built in correspondence with the base of the preliminary lining to act as springing for casting the vault in place and allowing the following excavation of the lower bench. Based on historical documents, the final lining was designed to be 0.9 m to 1.1 m thick at the crown and the invert and 1.3 m to 1.5 m thick at the springlines, depending on the tunnel chainage and the standard section adopted. Besides lining geometry, these also differ based on the presence and positioning of the steel rebars. Regional geological mapping examination and on-site geognostic surveys highlighted that the Olimpia tunnel passes through the Marne di Sant'Agata Fossili (AGA) formation for almost its entire length, as shown in Fig. 2. This is composed of marls and is scattered by clayey lenses or calcareous beddings as a function of depth. At the tunnel depth, the AGA formation is practically dry, except for localised and temporary seepage associated with rainfall infiltration.

Following the *Tunnel Assessment Program* put into practice by *Autostrade per l'Italia S.p.A.* since 2020 (Agresti et al., 2022; Mazzola et al., 2023), the Olimpia tunnel underwent deep inspections and a longitudinal georadar survey. The former revealed inner voids, honeycombing and deterioration of the construction joints (most of which occurred during the original concreting phase), spalling of the concrete cover with corrosion of steel reinforcements, widespread but closed cracks and water ingress, but limited to some humidity traces strewn all along the tunnel length. Similarly, the latter detected the presence of vertical and horizontal cracks, as well as some isolated cases of voids in the lining. The post-processing of data made it evident that about 50% of the intrados of the right tube of the Olimpia tunnel was characterised by the presence of defects. Therefore, an experimental campaign, including both on-site and laboratory testing, took place.

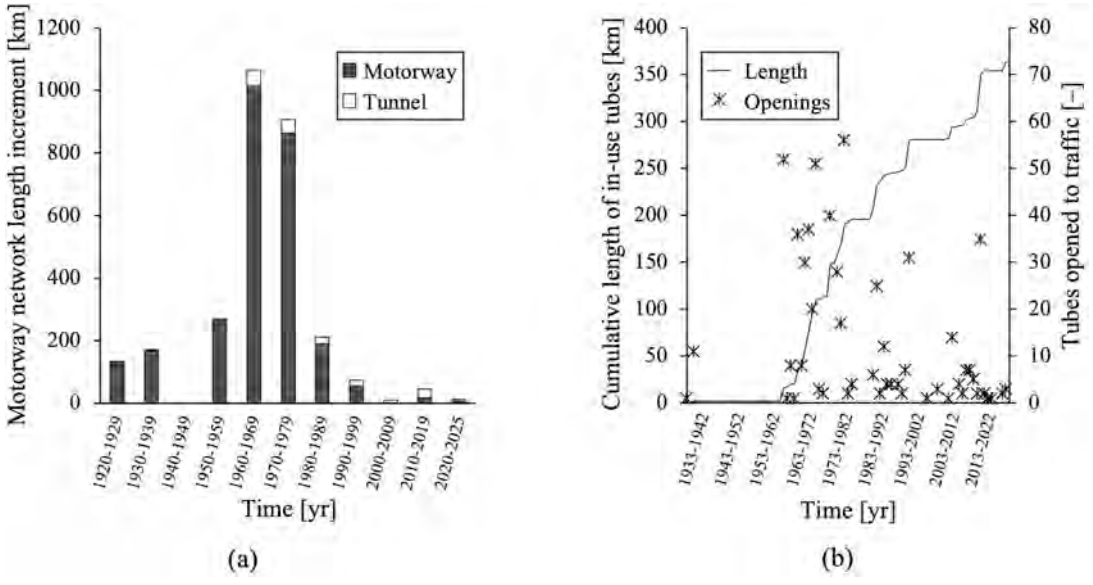

Fig. 1. *Autostrade per l'Italia S.p.A.* a) network length evolution and b) number and length of tubes opened to traffic.

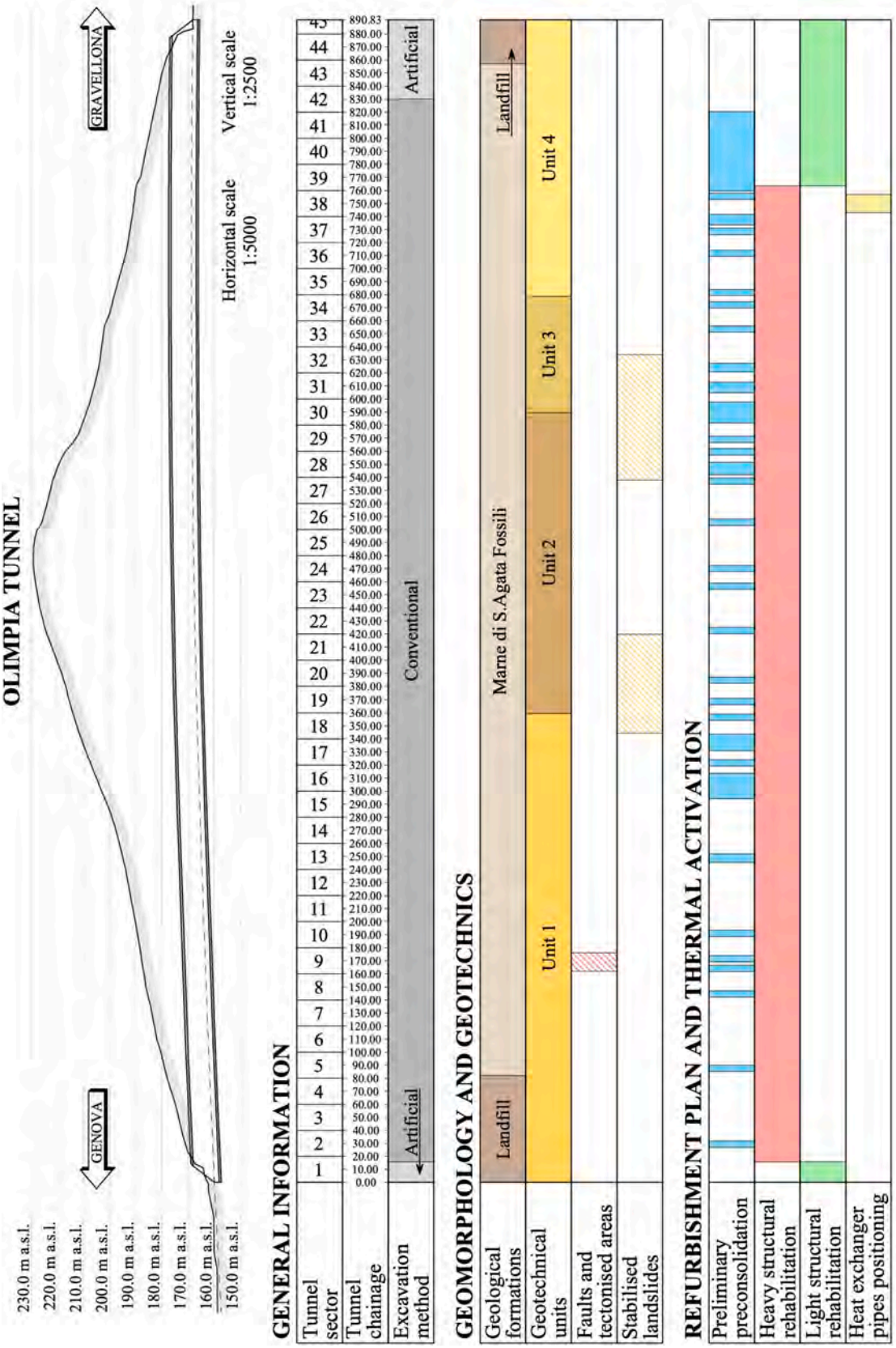

Fig. 2. Longitudinal profile of the Olimpia tunnel and corresponding general, geological, geotechnical and refurbishment information along the tunnel chainage.

On-site testing results verified the modest state of preservation of the Olimpia tunnel right tube. Specifically, transversal georadar surveys and video-endoscopy examinations highlighted the presence of voids inside the lining and sparse concrete thickness deficiencies along the tunnel length. Moreover, ultrasonic tomography confirmed further georadar survey outcomes, thus confirming average crack persistence of 30.0–50.0 cm along the lining thickness. Despite this, unconfined compression tests revealed an overall competent concrete material with an average compressive strength of about 20.0 MPa, and flatjack tests proved the final lining to be systematically unloaded along the entire tunnel length with a maximum hoop stress of less than 0.5 MPa. At the same time, laboratory testing allowed the geotechnical characterisation of the AGA formation, which was subdivided into four units (see Fig. 2) whose geotechnical parameters are shown in Table 1.

Based on the above, a refurbishment plan for the right tube of the Olimpia tunnel was designed and realised. As exemplified in Fig. 2, this consisted of light or heavy structural rehabilitation interventions, depending on the chainage, to renovate the existing tunnel lining to different extents.

About 750.0 m of the right tube of the Olimpia tunnel underwent heavy structural rehabilitation. This intervention aims to install a waterproofing system and replace part of the existing tunnel vault with a reinforced concrete intrados shell without involving the invert arch or modifying the original global static scheme of the structure (Mazzola et al., 2023) and providing a nominal service life extension of 50 years.

The rehabilitation intervention envisages the implementation stages listed in the following and depicted in Fig. 3. The workflow between stages 3 and 8 was performed for longitudinal sections of 6.0 m at a time, thus not markedly affecting the state of stress of the existing lining and allowing concurrent implementation in different sections along the tunnel.

- Stage 1 – preliminary pre-consolidation of the tunnel vault through fibreglass dowels, thus ensuring worker safety towards local block detachments.
- Stage 2 – demolition of the sidewalks to uncover the base of the springlines.
- Stage 3 – partial demolition of the existing lining over the entire vault through mechanical milling or hydro-demolition for an overall thickness of 35.0–40.0 cm.
- Stage 4 – removal of potentially unstable blocks, regularisation of the tunnel wall with a 3.0–5.0 cm thick sprayed concrete layer and installation of steel rebars to solidly connect the base of the intrados shell to the existing inverted arch.
- Stage 5 – cast in place of capping beams to act as a foundation for the shell.
- Stage 6 – installation of the waterproofing and drainage systems.
- Stage 7 – positioning of pre-assembled steel lattice ribs by hanging them to eyebolts fixed into the existing lining to act as reinforcement inside the shell.
- Stage 8 – cast in place of the reinforced concrete intrados shell.
- Stage 9 – deep renovation of the motorway structure, consequent roadbed lowering compliant with the in-force legislation about the required clearance dimension and assembly of the facilities running through the sidewalks.

Table 1
Geotechnical characterisation of the different geotechnical units identified along the Olimpia tunnel length.

Geotechnical parameters	Unit 1	Unit 2	Unit 3	Unit 4
Unit volume weight [kNm^{-3}]	20.0	18.7	19.6	19.2
Water content [%]	25.72	20.00	24.00	22.00
Plasticity index [%]	26	24	37	32
Overconsolidation ratio [-]		1.5–2.0		
Effective friction angle [°]	26	23	23	24
Undrained cohesion [kPa]	60.0	77.0	141.0	98.0
Deformability modulus [MPa]	44.0	149.0	51.0	37.0
Edometric modulus [MPa]	26.0	–	48.0	11.0
Shear modulus [MPa]	33.0	111.0	38.0	28.0
Hydraulic conductivity [mmd^{-1}]	0.035	–	–	–

The rehabilitation workflow ends with the intrados whitening up to 4.0 m from the motorway surface for visibility reasons.

The waterproofing installation methodology chosen is briefly described in the following, as it was a major concern for the thermal activation of the Olimpia tunnel at the design stage. The system consists of polyvinyl chloride (PVC) sheeting coupled with a geotextile layer, as shown in Fig. 4a. Such PVC sheeting is installed through fixing bands, preliminarily nail-gunned along the tunnel wall, generally in a transversal direction, as depicted in Fig. 4b. These act as grasping elements able to sustain the 2.1 m wide PVC sheeting modules, which are thermo-welded at the lateral edges to produce seamless waterproofing. The resulting system also admits using structural anchorages passing through the sheeting itself. This is the case of the eyebolts needed for steel lattice ribs positioning. Indeed, these are installed by using a fast-setting chemical resin with the twofold aim of structural support and hole sealing.

For the sake of completeness, the light structural intervention planned in correspondence with the entrances, instead, envisages replacing and restoring the tunnel intrados for a shorter thickness, including corroded steel reinforcements. This aims at mitigating the risk related to local block detachments without providing specific further overall structural strength with respect to the current tunnel lining conditions. Such an intervention will not be a matter of discussion in the present paper.

3. Description of the prototype

During the rehabilitation of the right tube of the Olimpia tunnel, a 14.0 m long section at about 150.0 m distance from the Gravellona-side portal (see Fig. 2) was instrumented for heat exchange. To this purpose, the solution referred to as *Extrados Energy Mats* by De Feudis et al. (2024) was selected, as perfectly fitting the aforementioned rehabilitation workflow, and implemented after the demolishing phase (Stage 3).

3.1. Site implementation

PE-Xa pipes (20.0 × 2.0 mm) were arranged in a transversal meandering pattern along four parallel hydraulic circuits, with a spacing of 40.0 cm, following the schemes depicted in Fig. 5 and Fig. 6. These were embedded within the non-structural regularisation layer, between the existing and the renovated tunnel vault and behind the waterproofing and drainage systems. This modus operandi prevents pipes from affecting the structural integrity of the intervention and minimises thermal stresses and strains in the intrados shell. The latter holds because of the insulating properties of the waterproofing sheeting that also reduce the impact of the aerothermal conditions of the underground environment on heat exchange. Since the Olimpia tunnel is expected to be a cold tunnel, this feature may prove to be paramount to allow proper geothermal exploitation. Moreover, the pipe spacing was appropriately selected as a compromise between maximising heat exchange efficiency and ensuring safe installation, avoiding interference with the eyebolts (Fig. 5b). Such a pipe arrangement also permits easy management of unlikely disruptions, as potential heat carrier fluid losses would be funnelled towards the drainage system by the waterproofing.

Some expedients were put into practice to allow the correct installation of pipes and minimise their possible interferences with the eyebolts and nails for steel ribs positioning and waterproofing sheeting setup, respectively. To the former aim, six longitudinally wall-attached metal rods were used to correctly pre-position pipes, as depicted in Fig. 7, that were subsequently fixed on the tunnel wall through metal

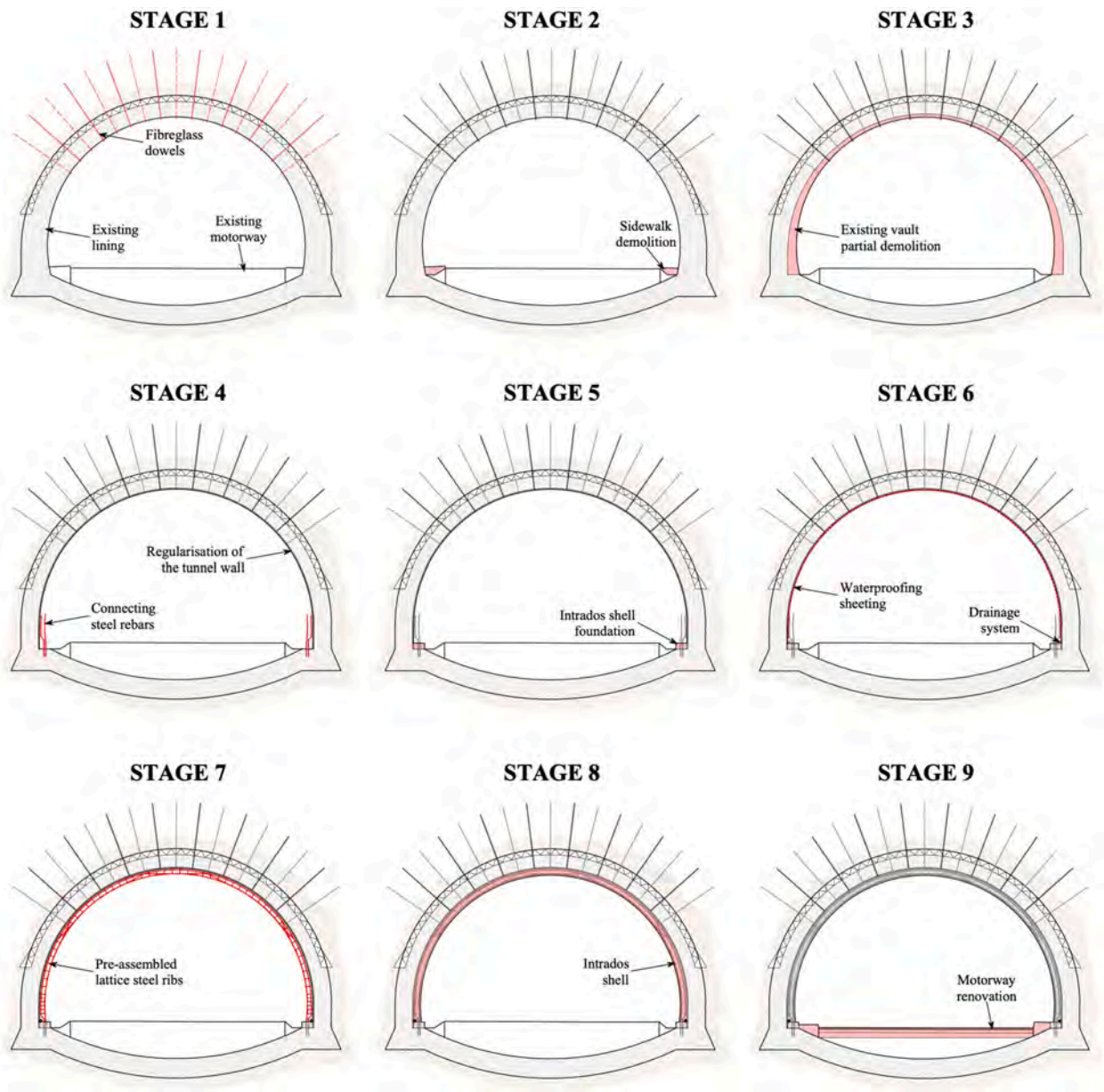

Fig. 3. Transversal cross-section view of the different rehabilitation intervention stages of the Olimpia tunnel.

clamps with a 1–2 pcs.m^{-1} frequency. To the latter, plastic cable clips were tied to the pipes with the same frequency as clamps to identify their position after spraying the regularisation layer, as illustrated in Fig. 8.

After pipe fixing, a preliminary 2.0-hour pressure test was performed to check for dowelling-related damage. Pipes were temporarily filled with plain water at 1.5–3.0 bar, and the pressure loss was evaluated at about 0.1 bar. This was endorsed to minor leaks at both ends of each subcircuit due to temporary hydraulic fittings.

Henceforth, the rehabilitation workflow envisaged for the Olimpia tunnel continued as described above (see Fig. 3). Attention was paid to nail-gun waterproofing fixing bands between pipe branches, thus avoiding ruptures, as shown in Fig. 9, and saving space for pipe housing through the lateral capping beams for the connection with the collectors. The renovation of the 14.0 m long thermally activated lining portion concluded with the steel ribs positioning and intrados shell cast in place, as depicted in Fig. 10.

The heat harnessed through geothermal exploitation is transferred for about 150.0 m in both directions along the tunnel by means of collectors running within the new sidewalks, coherently with the transversal footprint of the other facilities (fire protection system, optical fibre cables, etc.). To this end, jacketed pre-insulated PE-Xa collectors (32.0 × 3.0 mm) were laid in the sidewalk moulds, as depicted in Fig. 11a. The 30.0 mm thick insulation foam (see Fig. 11b), characterised by a thermal conductivity of 0.02 Wm^{-1}K^{-1}, should allow the heat carrier fluid to travel with negligible heat losses. To have access to maintenance points to the geothermal serpentine, eight precast inspection manholes were set along the thermally activated section. Herein, the inlet and outlet of the corresponding geothermal subcircuit connect to the return and supply collectors through ball valves, which enable full disconnection among such subcircuits.

The heat thus transferred is planned to be used for preventing the development of hoar frost during winter (anti-icing) on a 27.0 × 3.6 m stretch of the emergency lane outside of the Gravellona-side tunnel portal (see Fig. 2). On the contrary, in summer, the same motorway stretch is envisaged to function as a solar collector to retrieve thermal energy from solar irradiance to be stored in the geological formation behind the tunnel lining. Hence, according to the scientific terminology in the field (Mirzanamadi et al., 2018a,b; Mirzanamadi et al., 2019 and

Fig. 4. Details of the waterproofing system: view of the a) double-layer structure and b) fixing bands transversally nail-gunned along the tunnel wall.

Johnsson & Adl-Zarrabi, 2019, 2020, among others), the motorway pavement will behave as a hydronic heated pavement (HHP) in winter and a pavement solar collector (PSC) in summer.

For this purpose, the same PE-Xa pipes (20.0 × 2.0 mm) used for the thermal activation of the lining were also employed for instrumenting the motorway pavement. Consistent with the results of a sensitivity study carried out by De Feudis et al. (2026) aiming to thermally optimise the pipes arrangement, these pipes were installed in a transversal meandering pattern with a spacing of 30.0 cm, paying attention to leaving a 50.0 cm margin from the adjacent slow lane, following the schemes shown in Fig. 12 and Fig. 13.

This configuration envisages piping bending in correspondence with the lateral edges of the emergency lane. The rationale is threefold: from the hydraulic viewpoint, in the perspective of a future scale-up, this layout allows for fewer pipe bends, thus reducing hydraulic head losses and running costs. Then, from the structural viewpoint, Zhou et al. (2021) revealed that mechanical and thermal stresses accumulate at pipe bends, thus affecting the structural performance of the pavement. Accordingly, the layout chosen would distance such weak points from the central portion of the lane, where vehicles are most likely to transfer load. Finally, from the thermal viewpoint, a uniform thermal gradient in the travelling direction would be generated, thus avoiding differential slipping between same-axle vehicle wheels.

The motorway pavement was preliminarily milled for 14.0 cm, and then the pipes were fixed onto the surface, as depicted in Fig. 14. After, a 5.0 cm thick concrete slab (see Fig. 14c) was poured to cover and protect the serpentine for the subsequent binder (5.0 cm) and wearing (4.0 cm) asphalt layer setup (see Fig. 14d). Indeed, hard-grade asphalt mixtures need to be spread and compacted while hot (around 150.0°C), which would have damaged the piping permanently in the absence of such a concrete slab. Similar to the thermally activated lining portion, pipes were arranged to assemble four parallel circuits fully hydraulically dissectible through ball valves placed into eight cast-in-place inspection manholes.

The anti-icing solar-collecting geothermal system was finally connected to a hydraulic pump able to make the heat carrier fluid (propylene glycol–water mixture 20% by volume) flow within the parallel geothermal serpentines at about 0.36 m^3h^{-1} each, yielding a total system flow rate of around 1.44 m^3h^{-1}. Heat exchanger and collector piping diameters were selected according to hydraulic design criteria in order to ensure the required flow rate, resulting in a Reynolds number of about 4000 within the heat exchangers. In this way, hydraulic transient turbulence was achieved, thereby enhancing heat exchange without severely increasing running costs. The system does not envisage the presence of a Ground Source Heat Pump (GSHP), thus operating in free-heating and free-cooling modes during winter and summer, respectively.

To carry out all the above, an additional work burden of 30–40 man-hours (a work shift considering 3–4-man teams) was assessed for each subcircuit arranged within the tunnel vault (about 250.0 m of pipe). These are the results of workers fixing heat exchanger pipes using mobile elevating work platforms and dowelling the clamps with two plugs each. Using ad hoc working platforms and nail-gunning the clamps was estimated to reduce up to 50% of the installation time. Regarding the external portion, instead, an additional work burden of 8–10 man-hours (half of a work shift, considering 2-man teams) was assessed for each subcircuit.

The thermo-physical properties of the newly built intrados shell, the existing tunnel lining, the shotcrete regularisation layer, and the protection concrete slab embedding the piping within the HHP/PSC were determined through laboratory testing in compliance with ASTM D5334–22 and ASTM D7984–16. The campaign revealed that the existing lining features the highest thermal conductivity (1.86 $Wm^{-1}K^{-1}$) and capacity (2.81 $MJm^{-3}K^{-1}$), while the other materials tested exhibited slightly lower, but consistent values. Further details are reported in De Feudis (2025) and De Feudis et al. (2025).

3.2. Monitoring and automation system

After closing the hydraulic circuit and connecting it to a multistage in-line hydraulic pump, the whole system presents itself as shown in Fig. 15.

A comprehensive monitoring system was installed to assess the aerothermal conditions of the underground environment, the thermal behaviour of the newly built intrados shell and HHP/PSC, and the amount of heat dissipated/harnessed through the latter. Moreover, the internal and external air temperature is measured, too.

A total of twelve PT1000-A temperature transducers were installed to measure the temperature of the tunnel lining and road pavement, with six deployed on the tunnel side and six on the road side. Such transducers, with an accuracy of ±0.3°C, are wired to dataloggers (one for each triplet of transducers), which operate with a data acquisition interval of 10.0 minutes and, in turn, wirelessly communicate to an ethernet gateway (located in a shelter hosting the entire control system) able to upload monitoring recordings on a dedicated web service

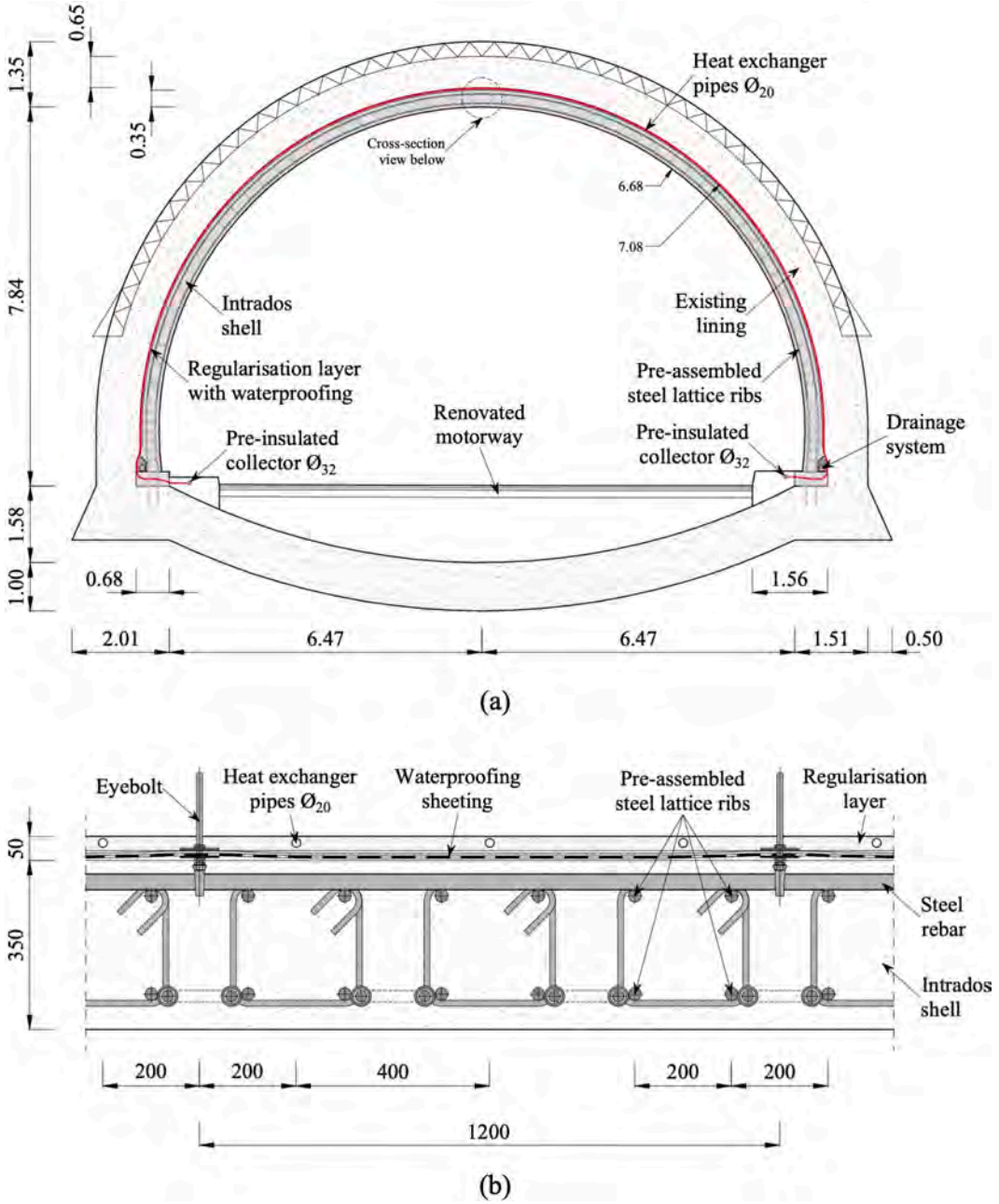

Fig. 5. A) transversal cross-section of the heat exchanger pipe arrangement (scale1:150) and b) longitudinal detailed profile of the eyebolts-pipe interaction (scale 1:15) of the energy retrofitting solution employed to thermally activate the Olimpia tunnel.

through a GSM router. Each of these dataloggers embeds a NTC10KΩ temperature sensor, able of recording ambient air temperature with an accuracy of ±0.2°C. The velocity of the mass air flowing within the tunnel, instead, is measured through an EE650 air velocity sensor, with an accuracy of ±0.2 ms^{-1}. This was dowelled on the tunnel intrados at 4.5 m above the slow lane sidewalk in a way to not interfere with the clearance gauge and detect, as accurately as possible, the movement of air induced by passing vehicles.

To evaluate the amount of heat dissipated/harnessed through the HHP/PSC during operation, two measuring points were envisaged along the collector's path within the Olimpia tunnel. Each of them is composed of an MS501 flow meter, a pair of PT500-B temperature transducers and an MV311 heat meter, which integrates the readings of the other two components over time to compute the thermal energy, with a data acquisition interval of 5.0 minutes and an overall accuracy of ±0.2%. Since the hydraulic circuit is closed, a measuring point would have been enough, assuming that collectors transfer heat without losses. However, two of them were installed on purpose to validate the second assumption, from the perspective of future applications.

The anti-icing solar-collecting prototype is designed to run automatically based on the monitoring system's recordings, specifically the temperature of the motorway pavement at around 2.0 cm depth from the surface. This is achieved through a hydraulic pump, made "smart" by integrating a Programmable Logic Controller (PLC). Whenever the temperature of the pavement goes below 3.0°C during winter, and above 30.0°C during summer, the PLC activates the system that heats up or cools down the road surface. Based on the needs, the PLC is also able to operate on the hydraulic pump power, thus modifying the fluid flow rate up to approximately 2.0 m^3h^{-1}.

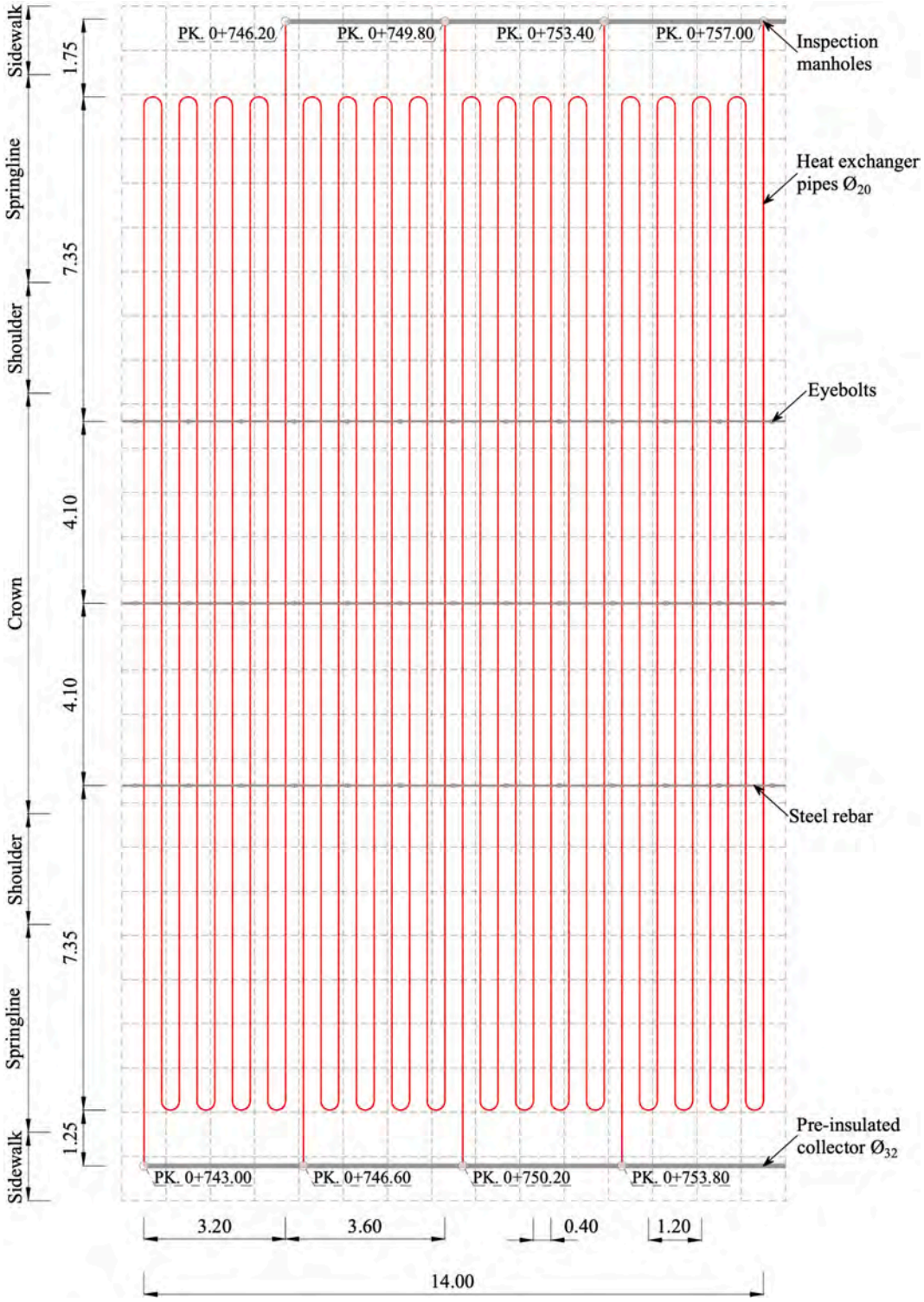

Fig. 6. Expanded view of the thermally activated vault of the Olimpia tunnel, represented in a 1.0 × 1.0 m grid (scale 1:150).

3.3. Start-up of the system

3.3.1. Hydraulic pressure tests

Upon completing the prototype's realisation, hydraulic pressure tests were carried out to inspect the integrity of the heat exchanger pipes and the watertightness of the hydraulic connections deployed along the hydraulic circuit. Compliant with UNI EN 806–4:2010, after flushing the air out of the pipes, the hydraulic circuit was gradually pressurised until a testing pressure that exceeded the maximum design value by 10%. This threshold has been conservatively assessed at 2.7–2.8 bar, so a testing pressure of about 3.0 bar was selected.

The first test lasted 40.0 hours. Throughout the testing process, the pressure dropped by about 0.7–0.8 bar from the initial measurement of 3.1 bar. All the inspection manholes hosting hydraulic fittings and valves or monitoring instrumentations were systematically inspected to verify their integrity, and no leakages were found along the circuit. Subsequently, a follow-up test lasting 2.5 hours was conducted, which resulted in a pressure reduction of 0.1 bar from the initial measurement

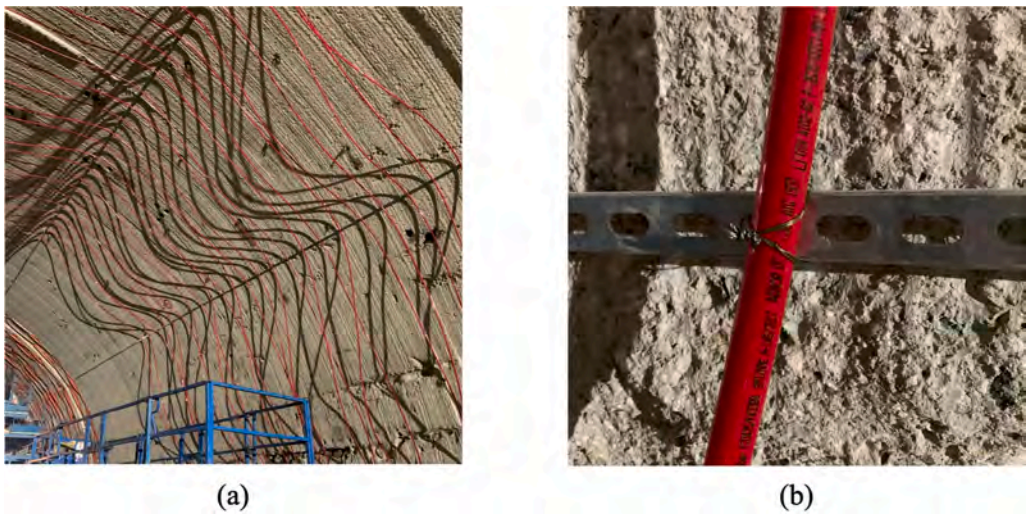

Fig. 7. Pipe pre-positioning through longitudinally wall-attached metal rods: a) view of the left springline and b) detail of the pipe-rod connection with metal wires.

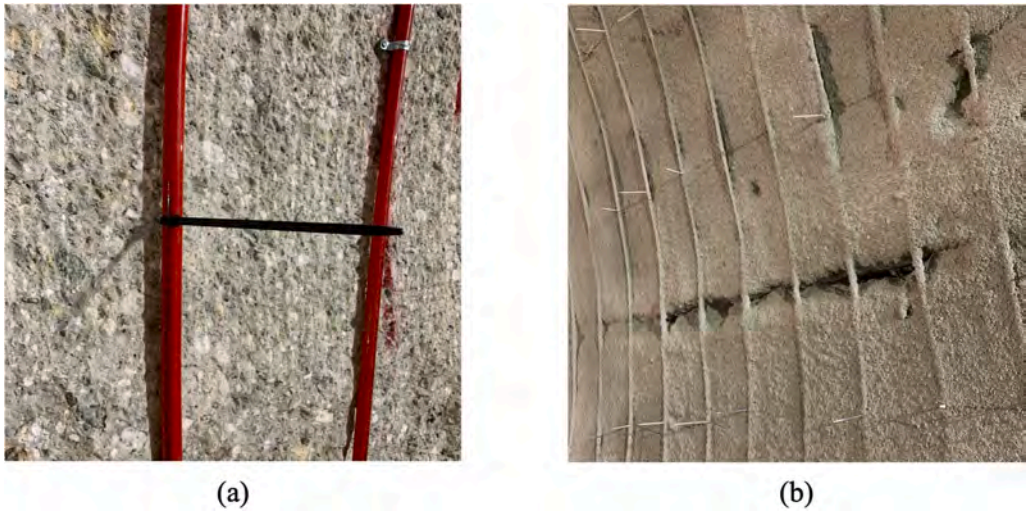

Fig. 8. Pipe equipped with plastic cable clips: view of the coil a) before and b) after spraying the regularisation layer.

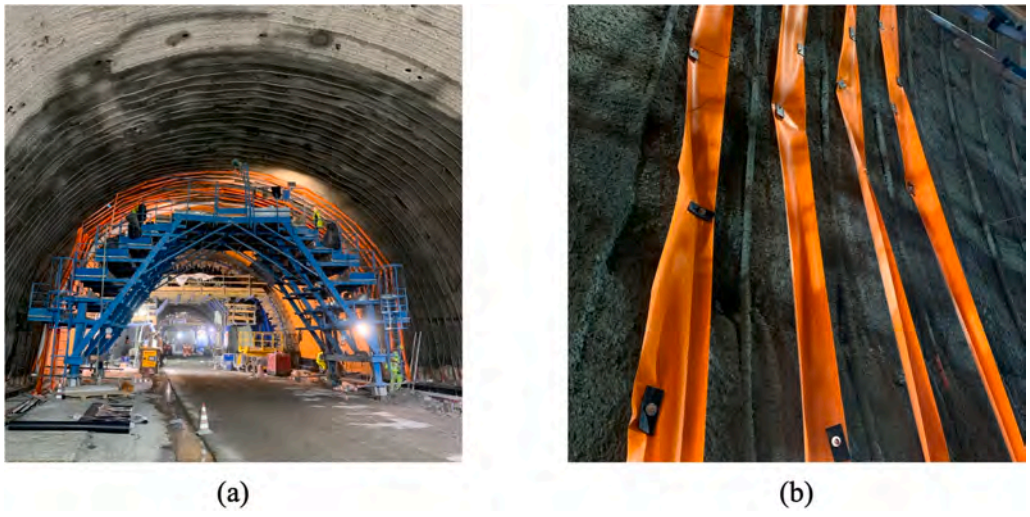

Fig. 9. a) Working platform used to install the waterproofing layer, and b) fixing bands nail-gunned along the tunnel wall, between heat exchanger pipe branches.

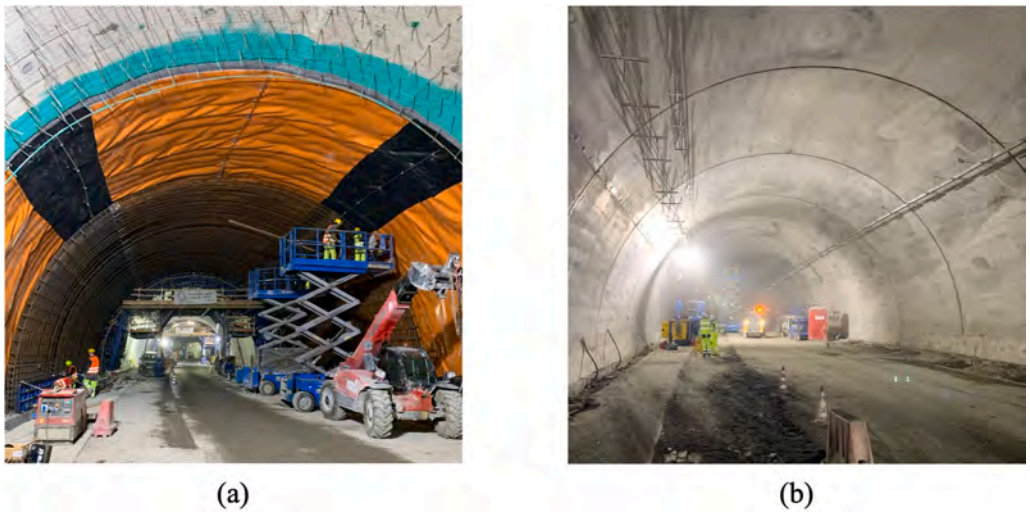

Fig. 10. The Olimpia tunnel thermally activated portion after a) positioning the pre-assembled steel lattice ribs and b) casting in place the intrados shell.

Fig. 11. Jacketed pre-insulated PE-Xa collector pipe: a) positioning within the sidewalk mould and b) cross-sectional view.

of 2.8 bar. After this, the system was pressurised to 3.1 bar, and the pressure drop was re-evaluated after 20.0 days. At that time, the analog manometer recorded a pressure of 2.0 bar. The testing outcomes just outlined are depicted in Fig. 16.

Notwithstanding the pressure drops experienced by the hydraulic piping during testing, two significant and encouraging conclusions may be drawn. On the one hand, the non-zero pressure measurements at the end of the tests indicate that the piping has not sustained any macroscopic damage or leakages that otherwise would have zeroed the readings of the manometer. This finding is consistent with the results of the preliminary pressure tests, which highlighted the integrity of the tunnel-side geothermal piping following the most damage-prone phase of the rehabilitation workflow (i.e., the installation of the waterproofing sheeting). On the other hand, the non-zero long-term pressure reading and the dryness of the manholes prove the absence of microscopic damage or leakages that otherwise would have made the fluid pressure drop consistently in a period as long as 20.0 days. The experienced pressure drops are likely due to the viscoelasticity of the piping.

3.3.2. *Thermal response test*

After ascertaining the integrity of the entire geothermal system, a thermal response test was performed to validate the geothermal potential of the 14.0 m long thermally activated portion of the Olimpia motorway tunnel. Compliant with VDI 4640:2010, the thermal response test consisted of dissipating a known constant amount of heating power in the ground, in this case equal to 4.6–4.7 kW, and recording primarily the fluid inlet and outlet temperatures, but also the heat carrier fluid flow rate and the ambient temperature.

The test was run for 12.0 hours; at that stage, the above-mentioned monitoring system had not yet begun data acquisition. This duration was chosen because, unlike standard geothermal systems (VDI 4640:2010), the geothermal system is not intended to function regularly throughout the year, activating only when needed. Thus, mid-term results are more relevant than long-term data in this context. Throughout the testing process, the flow rate was kept constant at approximately 1.5 m^3h^{-1} with only imperceptible variations observed. The importance of this aspect cannot be overstated, as it is essential to validate the interpretation of hydraulic pressure tests and confirm the integrity of the system. Indeed, no additional pressurisation of the piping was required before starting the test. Notably, unlike conventional borehole heat exchangers, the meandering layout of the geothermal piping embedded in the tunnel lining precludes interpretation based on the Infinite Line Source (ILS) theory. Consequently, standard test outputs such as effective ground thermal conductivity or global thermal resistance of the system cannot be determined analytically. The test was, therefore, carried out primarily to support the start-up of the system and to

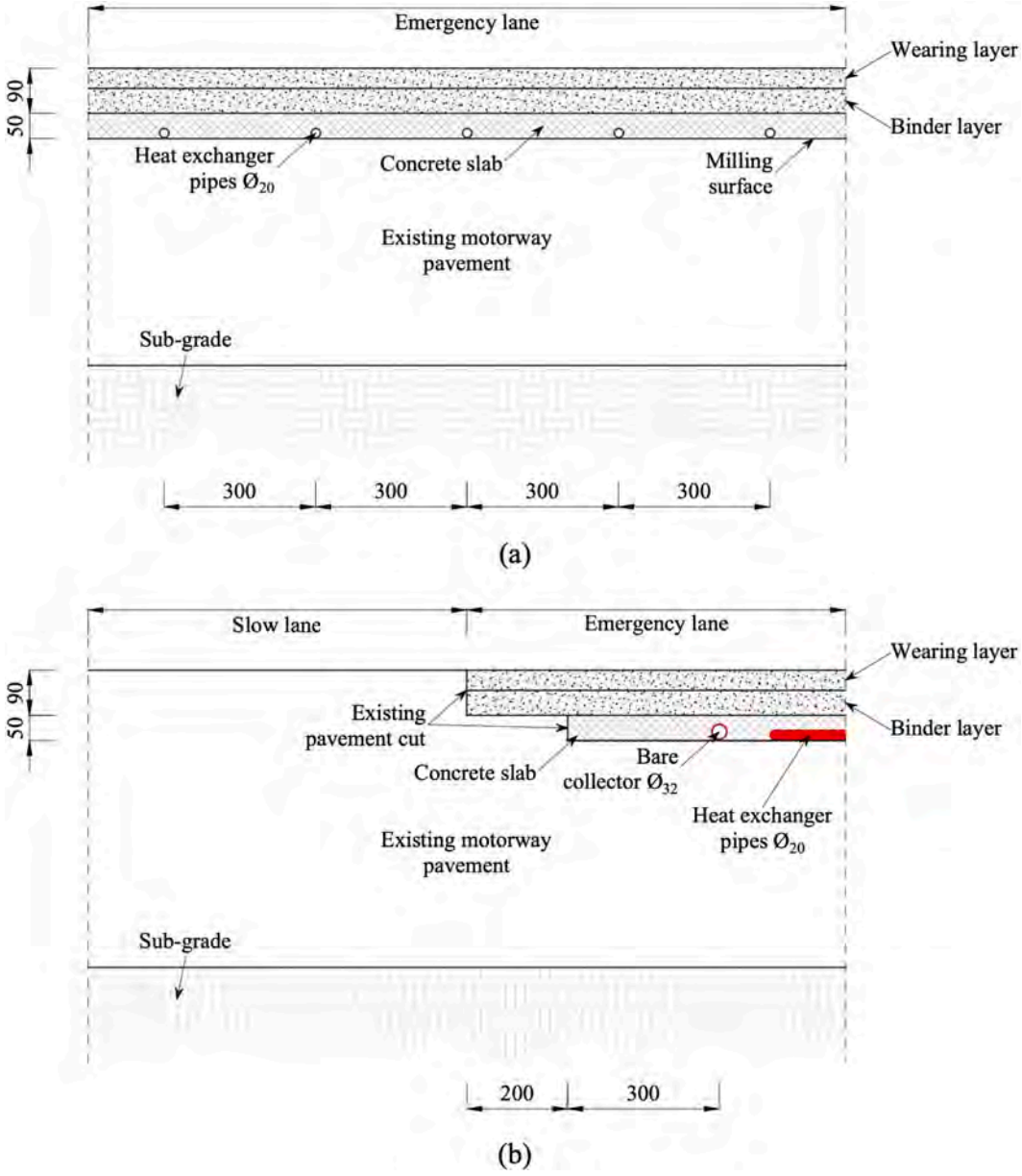

Fig. 12. a) Longitudinal and b) transversal cross sections of the motorway side heat exchanger pipe arrangement and the clearance between emergency and slow lanes, respectively (scale 1:15).

preliminarily assess its heat exchange potential under controlled conditions. The results of the thermal response test are shown in Fig. 17.

The initial temperature of the fluid coming from the geothermal coil arranged in the newly built lining of the Olimpia tunnel was attested at about 12.5°C for an initial duration of 10.0 minutes. In a standard thermal response test, this value tallies with the undisturbed temperature of the ground. Nevertheless, given the relatively shallowness of the pipes within the tunnel lining compared to the depth of more common borehole heat exchangers, it can be easily imagined that, despite the presence of the waterproofing layer, the temperature value stated above is also influenced by anthropogenic heat fluxes from inside the tunnel (Buhmann et al., 2016). It can be inferred that, given the timing of the test shortly after the end of the cold season, the undisturbed ground temperature is likely to exceed 12.5°C. This observation aligns with the thermal maps presented by Sethi et al. (2021), which indicate temperatures of approximately 13.6°C for the site of the Olimpia tunnel.

The Olimpia energy tunnel demonstrated the ability to inject 4.6–4.7 kW into the surrounding ground quite steadily. After experiencing an initial temperature rise of approximately 1.1°C in the first 30.0 minutes, the heat carrier fluid only heated up by about 1.6°C in the following 11.5 hours. Thus, accounting for an average inlet–outlet fluid temperature difference of 2.9°C, the energy tunnel section, in this specific test, worked at a geothermal efficiency per unit of thermally activated area of around 15.0 Wm^{-2}. Within the range of energy tunnel applications reported in the literature, this performance lies in the lower-to-middle portion of observed heat exchange rates, spanning from 10.0 to 40.0 Wm^{-2} (Salciarini et al., 2026). Higher values are commonly associated with extremely favourable groundwater or aerothermal conditions, whereas the moderate output recorded in the Olimpia tunnel reflects less advantageous hydrogeological and operational settings.

4. Operation of the system

4.1. Solar-collecting test

The first experimental campaign was conducted between July and

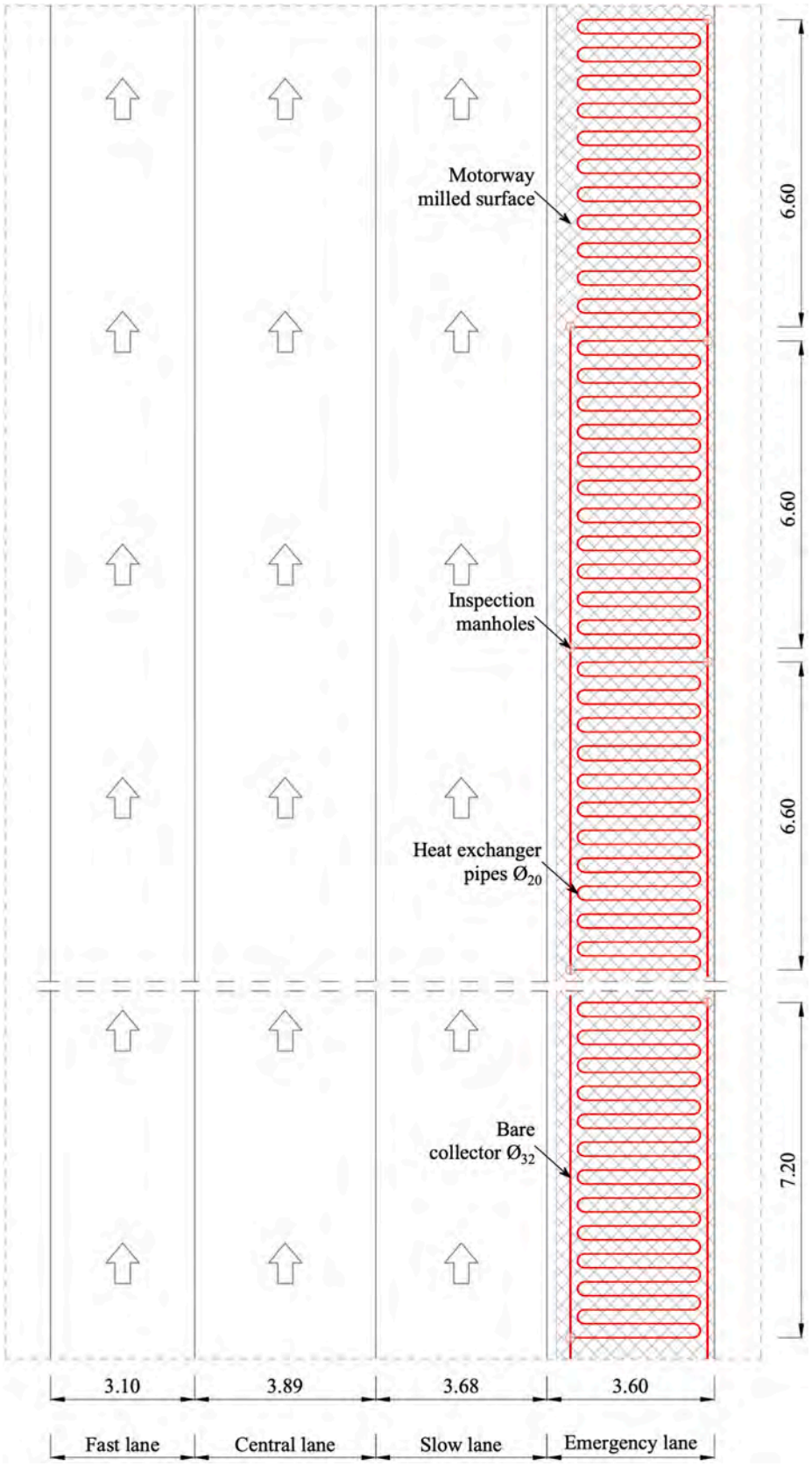

Fig. 13. Plan view of the HHP/PSC emergency lane stretch (scale 1:150).

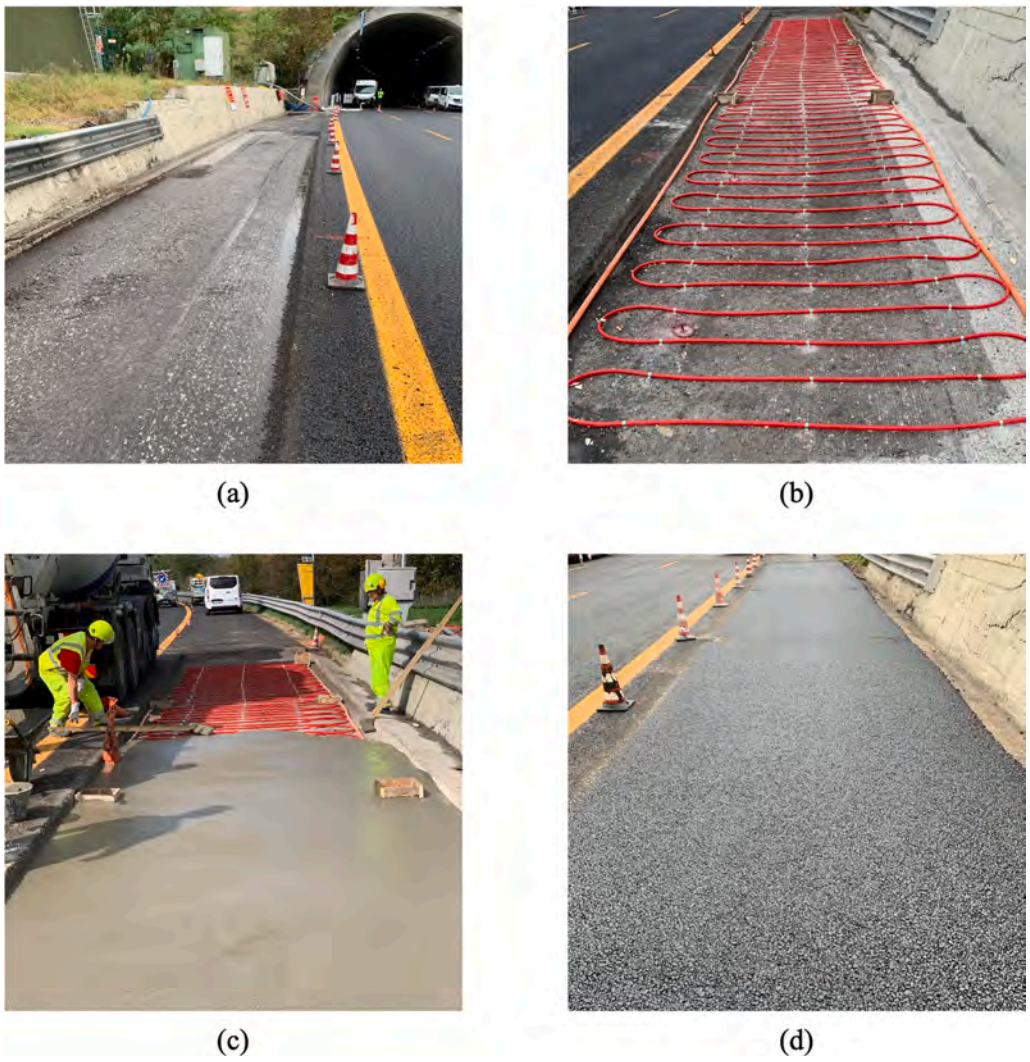

Fig. 14. a) Emergency lane after the milling operations, b) heat exchanger pipes arrangement and inspection manholes setup, c) concrete slab pouring and d) completely restored emergency lane.

September 2025 to assess the system's solar-collecting potential. During this period, temperatures in the newly constructed lining and the PSC were monitored, along with the heat harnessed through the latter and the ambient temperature within the tunnel structure. Unfortunately, data from the EE650 air velocity sensor were unavailable at that time. The results of a 16.5-day continuous solar-collecting test are depicted in Fig. 18.

The temperature data exhibited distinct daily cycles, most pronounced for the motorway pavement profile, which reached peak values of approximately 50.0°C, clearly reflecting the influence of solar irradiation. In contrast, the temperature of the tunnel lining, measured at depths of 7.0 cm, 14.0 cm, and 20.0 cm within the concrete element, showed progressively damped fluctuations with increasing depth, indicating the influence of the thermal inertia of the structural element. Notably, the inlet and outlet fluid temperatures of both the energy tunnel and the PSC displayed nearly identical values throughout the test, indicating negligible thermal losses along heat carrier fluid circulation path and confirming the effective insulation of the collector system. On average, an inlet–outlet temperature difference of 2.5°C was observed during the daytime peak hours.

Over the 16.5-day testing period, the geothermal system captured 1.1 MWh_t of solar energy through the PSC, achieving a maximum collection rate of 50.0 Wm^{-2}, totalling about 5.0 kW across the entire PSC area. Such a value corresponds to an injection rate on the energy tunnel side of approximately 10.0–15.0 Wm^{-2}, which is in agreement with the outcome of the thermal response test previously described.

With specific reference to the temperature difference between the piping-instrumented pavement area and the uninstrumented one, thermal imaging revealed an appreciably lower surface temperature in the former case, as evident in Fig. 19. Specifically, based on the image region closest to the camera that is the most reliable one for comparison reasons, the PSC section reached approximately 37.0°C, compared to 40.0–41.0°C in the adjacent conventional pavement. This temperature reduction of about 3.0–4.0°C demonstrates the system's capability to effectively limit surface overheating, thus contributing to the mitigation of pavement damage associated with rutting phenomena.

4.2. *Anti-icing test*

The follow-up experimental phase, spanning from December 2025 to January 2026, focused on evaluating the system's anti-icing capabilities. As in the previous case, monitoring encompassed temperatures within the newly installed lining and HHP, heat dissipated through the HHP, and tunnel ambient temperature, while EE650 air velocity sensor data remained unavailable. Unlike previous solar-collecting tests, this experiment operated intermittently, with the system activating automatically based on the measured HHP temperature. The activation threshold temperature, as anticipated in Section 3.2, was set at 3.0°C.

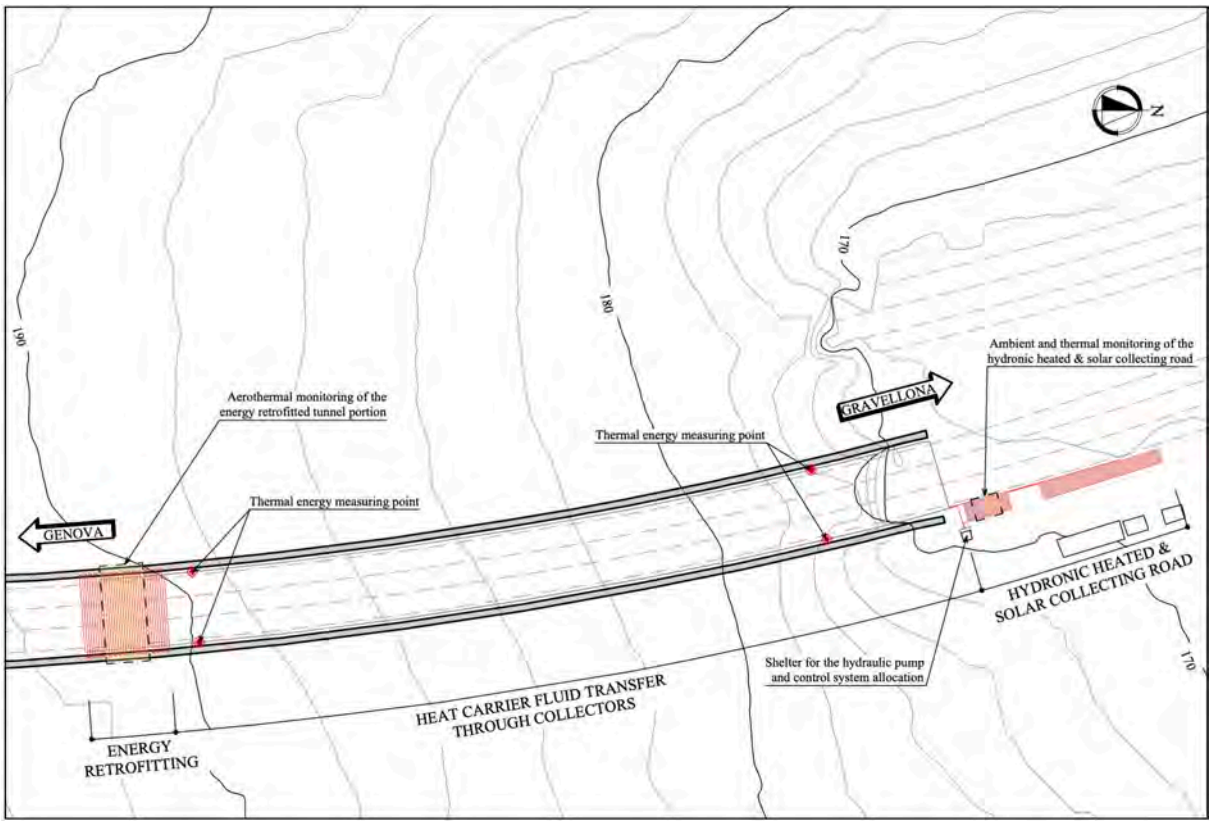

Fig. 15. Plan view of the geothermal system and of the monitoring instrumentation installed in the Olimpia tunnel (scale 1:1250).

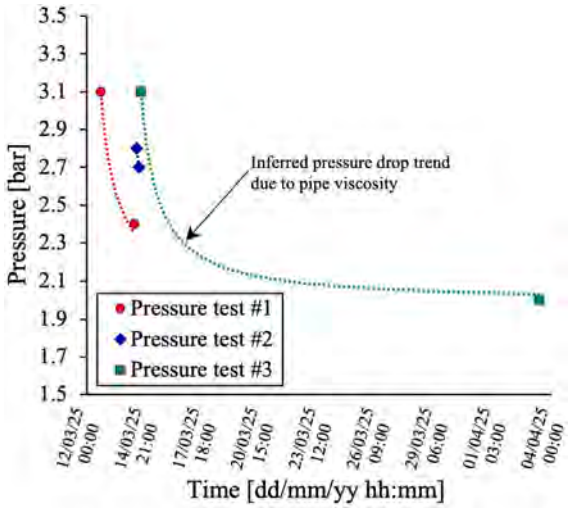

Fig. 16. Results of the hydraulic pressure tests carried out to check the integrity of the geothermal system.

When the temperature of the HHP fell below this threshold, the system operated at the design flow rate (i.e., 1.44 m^3h^{-1}) for active anti-icing. Above 3.0°C, a minimal circulation flow rate of 0.4 m^3h^{-1} was maintained to guarantee system readiness and monitoring over time. The intermittent anti-icing test, conducted over 17.0 days, yielded the results shown in Fig. 20.

Beyond the daily cycles, the temperature data also clearly exhibited distinct operational cycles corresponding to the intermittent working strategy, most pronounced in the thermal power profile, which precisely reflected the system's activation state. At the coldest point of the anti-icing test, the HHP dropped to around −2.5°C, while external ambient air temperature reached a temperature of −5.7°C, yielding a temperature elevation of approximately 3.0°C under these conditions. As also noticed in the previous test, the internal air temperature demonstrated an attenuated profile that mirrored the external temperature trend, with an average temperature shift of about 5.0°C. The inlet–outlet temperature difference of the heat carrier fluid averaged 1.3°C during active anti-icing operation and reached 1.8°C during the coldest hours of the test. During the test, the road surface fell below 0.0°C for only 50.0 hours, whereas the external air temperature remained below freezing for more than three times this duration.

Over the 17.0-day testing period, the geothermal system dissipated 649.1 kWh_t of thermal energy through the HHP, achieving a maximum heating rate of 30.0 Wm^{-2}, totalling around 3.1 kW across the entire HHP area. This corresponds to an extraction rate on the energy tunnel side of approximately 8.0–10.0 Wm^{-2}, which remains consistent with the outcomes of the previous thermal response test, considering the lower inlet–outlet fluid temperature difference observed in this case.

Regarding the temperature difference between the heated HHP area and the conventional pavement, thermal imaging revealed an appreciably higher surface temperature in the former, as shown in Fig. 21. The HHP section maintained a temperature of about 2.0°C, compared to 0.5°C in the adjacent conventional pavement. This temperature elevation of approximately 1.5°C, expected to increase with more severe environmental conditions, demonstrates the system's capability to effectively warm the motorway pavement, thus delaying or preventing hoar frost formation, thereby enhancing safety and mitigating freeze–thaw damage within the road structure.

5. Conclusions

This paper illustrates the first-ever existing tunnel section, systematically instrumented for heat exchange purposes during rehabilitation works following one of the energy retrofitting solutions proposed by De

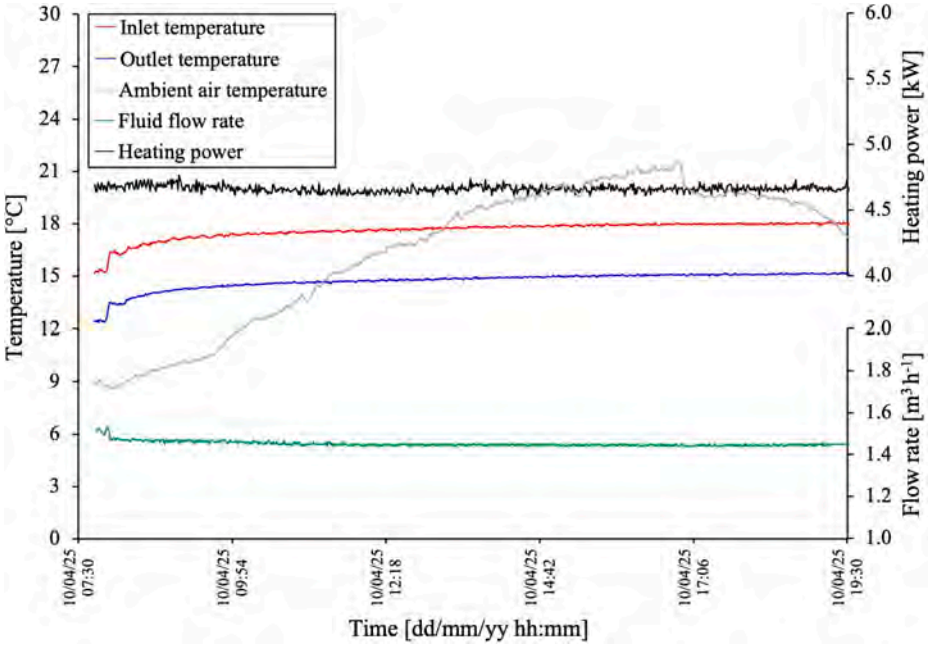

Fig. 17. Inlet and outlet heat carrier fluid and ambient air temperature, fluid flow rate and heating power data recorded during the thermal response test.

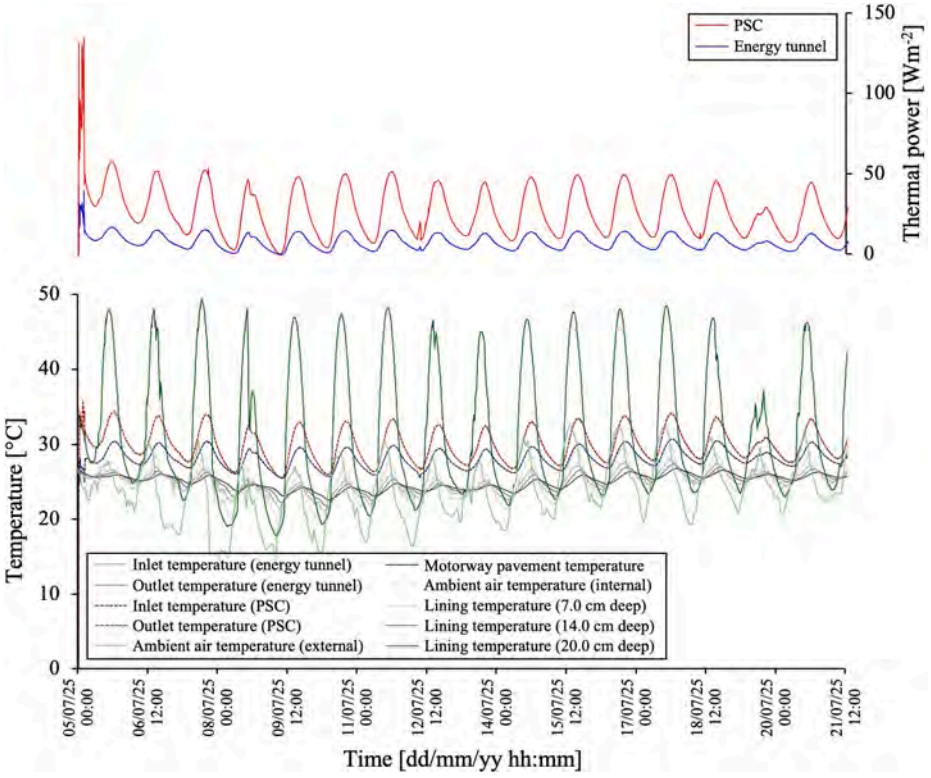

Fig. 18. Inlet and outlet heat carrier fluid (from both the energy tunnel and PSC), internal and external ambient air, tunnel lining (at different depths along its thickness) and motorway pavement temperature and cooling power data recorded during the 16.5-day continuous solar-collecting test.

Feudis et al. (2024). Among several open issues, the thermal activation of existing tunnel infrastructures had long represented a major research gap in energy tunnel technology that can now be considered fully addressed, having been successfully framed and constrained into a real tunnel rehabilitation workflow with no alterations to standard working practices and only minimal adjustments to the construction sequence. The feasibility of this retrofitting approach has been successfully demonstrated, requiring only relatively simple on-site operations. Notably, no specialised expertise is needed beyond the standard skill set that workers are typically expected to possess.

The energy tunnel implementation was then connected to an HHP/PSC to enable anti-icing operation during winter and solar thermal energy storage during summer. The integrity of the entire geothermal system was also guaranteed through hydraulic pressure testing, and a

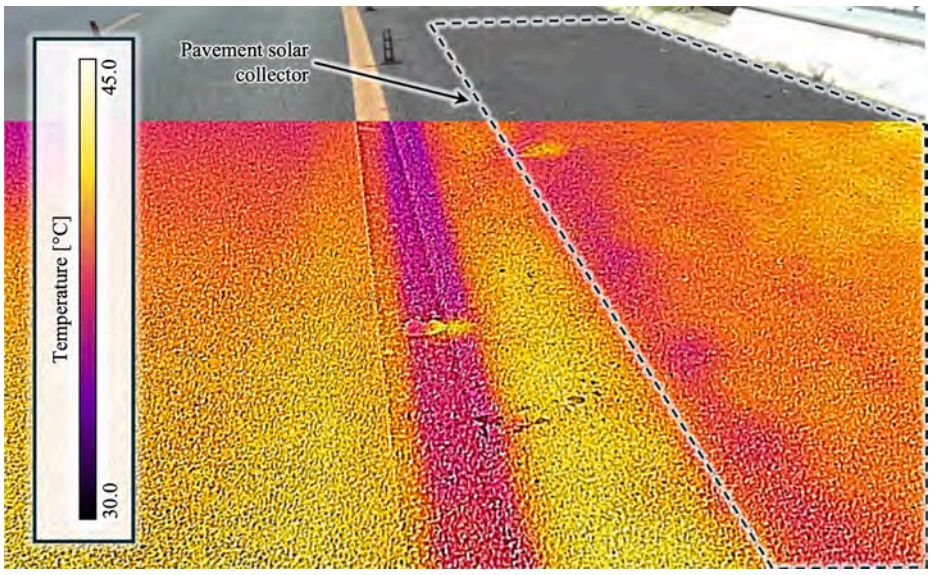

Fig. 19. Surface temperature distribution of the PSC obtained from thermal imaging on 8 July 2025 at 18:30.

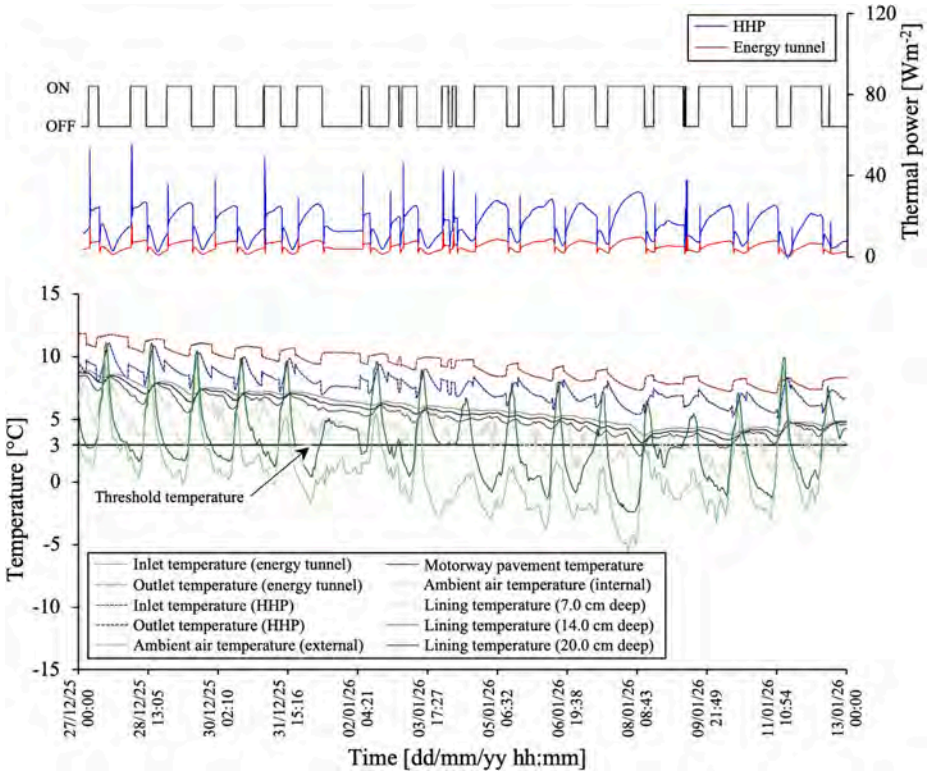

Fig. 20. Inlet and outlet heat carrier fluid (from both the energy tunnel and HHP), internal and external ambient air, tunnel lining (at different depths along its thickness) and motorway pavement temperature and heating power data recorded during the 17.0-day intermittent anti-icing test.

geothermal potential of about 15.0 Wm^{-2} was assessed through thermal response testing. The solar-collecting experimental campaign conducted between July and September 2025 conclusively demonstrated the operational reliability and energy-harvesting efficiency of the prototype in solar-collecting mode under real environmental conditions, confirming its ability to capture approximately 60–70 kWh_t of solar energy per day. Instead, the anti-icing experimental campaign carried out between December 2025 and January 2026 validated the frost-prevention capability of the prototype in anti-icing mode under real operational conditions, confirming its ability to maintain a temperature difference of approximately 1.5°C relative to unheated pavement sections. Overall, while both operational modes proved the system's technical viability, the free-cooling solar-collecting mode yielded superior performance, driven by the more favourable temperature differential between the solar-heated pavement and the ground. The free-heating anti-icing mode, although already demonstrating meaningful frost-prevention potential in its current free-heating configuration, still leaves room for further enhancement through two targeted developments: the optimisation of the embedment depth of the piping within the pavement to improve upward heat transfer efficiency without jeopardizing structural

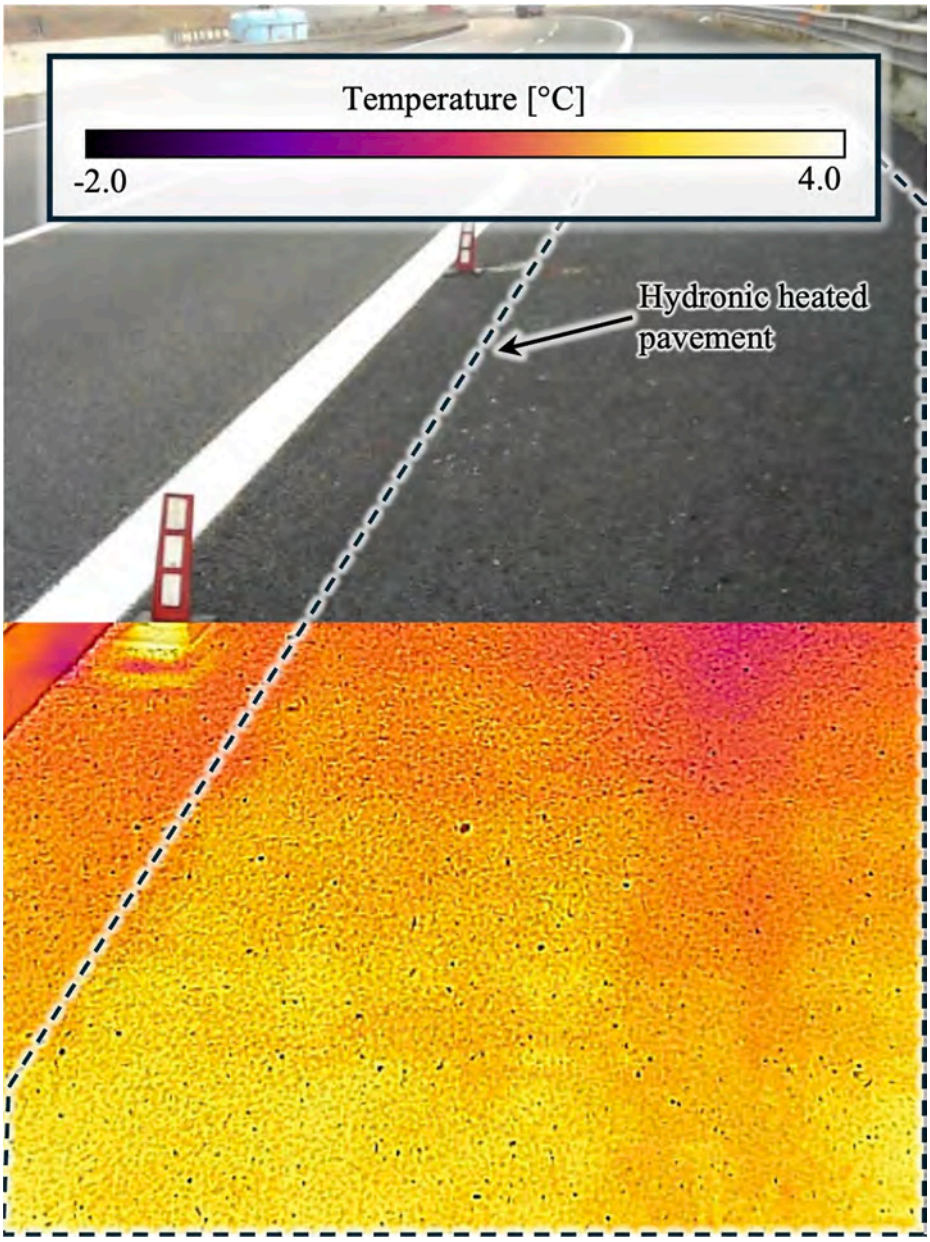

Fig. 21. Surface temperature distribution of the HHP obtained from thermal imaging on 27 January 2026 at 08:10.

integrity, and the integration of a GSHP to amplify the available thermal energy and unlock the full anti-icing potential of the system under more severe winter conditions.

In addition to demonstrating the feasibility and operational performance of the technology, the potential for scaling energy retrofitting, its cost-competitiveness, and environmental benefits have been assessed in related studies. De Feudis et al. (2024) and De Feudis (2025) estimated an average Levelized Cost of Heat (LCOH) of around 100–115 €MWh$_t^{-1}$, making geothermal energy from energy retrofitting economically comparable to conventional sources such as natural gas. In addition, with respect to the latter, geothermal energy is less exposed to price fluctuations and can reduce CO_2-eq. emissions by up to 60%. De Feudis et al. (2026) further evaluated the benefits of the large-scale deployment of energy tunnel-integrated anti-icing systems, reporting a Return On Investment (ROI) ranging from 12 to 15 years for a purposely selected 9.0 km stretch along the A26 motorway in Italy. Overall, systems like these embody a more environment- and infrastructure-friendly alternative to conventional de-icing salt spreading, which has detrimental impacts on infrastructures and vehicles, and may provoke substantial damage to vegetation and freshwater.

The experience gained from the Olimpia tunnel paves the way for fully unlocking the potential of sleeping geothermal facilities, such as existing tunnels, for a wide range of applications. These may include the heating and cooling of buildings, the reducing of ventilation requirements in hot tunnels, or even the implementation of anti-icing or de-icing systems for road pavements. As an illustrative case, considering only the motorway network managed by *Autostrade per l'Italia S.p.A.*, the thermal activation of existing tunnels could allow the exploitation of a total geothermal output in the range of 200–400 TWh$_t$. To put this figure into perspective, in 2022 Italy produced approximately 125 TWh$_t$ from renewable thermal energy sources (solar thermal, geothermal, aerothermal, hydrothermal, biomass, biogases and bioliquids).

CRediT authorship contribution statement

S. De Feudis: Writing – review & editing, Writing – original draft,

Visualization, Formal analysis, Data curation, Conceptualization. **A. Insana:** Writing – review & editing, Supervision, Conceptualization. **M. Barla:** Writing – review & editing, Supervision, Funding acquisition, Conceptualization.

Declaration of competing interest

The authors declare that they have no known competing financial interests or personal relationships that could have appeared to influence the work reported in this paper.

Acknowledgements

This study was carried out within the projects "NEST – Network 4 Energy Sustainable Transition" funded under the National Recovery and Resilience Plan (NRRP), Mission 4 Component 2 Investment 1.3 - Call for tender No. 1561 of 11.10.2022 of Ministero dell'Università e della Ricerca and "GEOREFIT – Closing knowledge gaps on energy geo-structures for retrofitting of buildings and infrastructures" funded by the Ministero dell'Università e della Ricerca within the PRIN 2022 program (D.D.104 -02/02/2022). This manuscript reflects only the authors' views and opinions and the Ministry cannot be considered responsible for them.

For the implementation of the prototype in the Olimpia motorway tunnel, the Authors are willing to acknowledge the help of the large number of people and companies that, in different ways, contributed to the project. The site installation was the result of an agreement set by the *Politecnico di Torino* with *Autostrade per l'Italia S.p.A*. In this respect, special thanks are devoted to Maurizio Mazzola, Greta Gualco, Luca Zilli, Federico Giunta, Marco De Meis, Alessandro Tonghini (from *Autostrade per l'Italia S.p.A.*), Lapo Baccolini, Alessia Zangari, Andrea Poli, Bushaj Selam, Alessandro Passuello (from *Tecne S.p.A.*) Giacomo Casanova (from *Amplia Infrastructures S.p.A.*), Andrea Zanelli, Marco Proietti, Vitantonio Caputo (from *CI.E.L. S.p.A.*) and Houssem Addine Bendjemaa (from *Italconsult S.p.A.*).

Data availability

Data will be made available on request.

References

Adam, D., Markiewicz, R., 2009. Energy from earth-coupled structures, foundations, tunnels and sewers. Geotechnique 59 (3), 229–236. https://doi.org/10.1680/geot.2009.59.3.229.

Agresti, F.S., Barla, M., Insana, A., Marchiondelli, A., Migliorino, P., Rosso, E., Selleri, A., Spina, B., 2022. Integrated approach for the inspection and special maintenance of italian motorway tunnels: the Scampitella case. Gallerie e Grandi Opere Sotterranee 141, 53–63.

Alvi, M.R., Insana, A., Barla, M., 2022. Thermal performance assessment of an energy lining for the Lyon-Turin base tunnel. Soils and Rocks 45 (1), 1–12. https://doi.org/10.28927/SR.2022.000722.

Atkinson, C., Paraskevopoulou, C., & Miller, R. (2021). Investigating the rehabilitation methods of Victorian masonry tunnels in the UK. *Tunnell. Undergr. Space Technol.*, *108*(November 2020), 103696. https://doi.org/10.1016/j.tust.2020.103696.

Barla, M., & Insana, A. (2023). Energy tunnels as an opportunity for sustainable development of urban areas. *Tunnell. Undergr. Space Technol*, *132*(November 2022), 104902. https://doi.org/10.1016/j.tust.2022.104902.

Barla, M., Di Donna, A., Insana, A., 2019. A novel real-scale experimental prototype of energy tunnel. Tunn. Undergr. Space Technol. 87 (January), 1–14. https://doi.org/10.1016/j.tust.2019.01.024.

Barla, M., Baralis, M., Insana, A., Aiassa, S., Antolini, F., Vigna, F., Azzarone, F., Marchetti, P., 2021. On the thermal Activation of Turin Metro Line 2 Tunnels. Lecture Notes Civil Eng. 126, 1069–1076. https://doi.org/10.1007/978-3-030-64518-2_127.

Bidarmaghz, A., Narsilio, G.A., 2018. Heat exchange mechanisms in energy tunnel systems. Geomech. Energy Environ. 16, 83–95. https://doi.org/10.1016/j.gete.2018.07.004.

Brandl, H., 2006. Energy foundations and other thermo-active ground structures. Geotechnique 56 (2), 81–122. https://doi.org/10.1680/geot.2006.56.2.81.

Buhmann, P., Moormann, C., Westrich, B., Pralle, N., Friedemann, W., 2016. Tunnel geothermics—A German experience with renewable energy concepts in tunnel projects. Geomech. Energy Environ. 8, 1–7. https://doi.org/10.1016/j.gete.2016.10.006.

Cousin, B., Rotta Loria, A.F., Bourget, A., Rognon, F., Laloui, L., 2019. Energy performance and economic feasibility of energy segmental linings for subway tunnels. Tunn. Undergr. Space Technol. 91 (June), 102997. https://doi.org/10.1016/j.tust.2019.102997.

De Feudis, S., 2025. Energy retrofitting of existing tunnels – from conceptualization to full-scale implementation. Ph.d. Thesis. Politecnico Di Torino. https://doi.org/10.13121/polito/porto/3001707.

De Feudis, S., Insana, A., Barla, M., 2024. Seizing the opportunity of energy retrofitting of existing tunnels. Tunn. Undergr. Space Technol. 154, 106109. https://doi.org/10.1016/j.tust.2024.106109.

De Feudis, S., Insana, A., & Barla, M. (2025). A solar-collecting system for tunnel thermal storage. *3rd Int. Conf. Energy Geotech. 2025*, 1–4.

De Feudis, S., Insana, A., Barla, M., 2026. Sensitivity analysis for the design optimisation of an energy tunnel based hydronic heated pavement. Transp. Geotech. 56, 101692. https://doi.org/10.1016/j.trgeo.2025.101692.

Di Donna, A., Barla, M., 2016. The role of ground conditions on energy tunnels' heat exchange. Geomech. Energy Environ. 3 (EG4), 214–224. https://doi.org/10.1680/jenge.15.00030.

Dornberger, S.C., Rotta Loria, A.F., Zhang, M., Bu, L., Epard, J.L., Turberg, P., 2022. Heat exchange potential of energy tunnels for different internal airflow characteristics. Geomech. Energy Environ. 30, 100229. https://doi.org/10.1016/j.gete.2020.100229.

Fava, A. R., Ghidoli, M., Carli, L., & Galvanin, P. (2019). Refitting strategies for Italian historical railway tunnels. *Tunnels and Underground Cities: Engineering and Innovation Meet Archaeology, Architecture and Art- Proceedings of the WTC 2019 ITA-AITES World Tunnel Congress*, 2071–2080. https://doi.org/10.1201/9780429424441-219.

Franzius, J. N., & Pralle, N. (2011). Turning segmental tunnels into sources of renewable energy. *Proc. Institut. Civil Eng.: Civil Eng.*, *164*(1), 35–40. https://doi.org/10.1680/cien.2011.164.1.35.

Frodl, S., Franzius, J.N., Bar, T., 2010. Planung und bau der tunnel-geothermieanlage in Jenbach. Geomechanik Und Tunnelbau 3 (5), 658–668. https://doi.org/10.1002/geot.201000037.

Grossauer, K., Modetta, F., Tanner, U., 2017. Die „Normalbauweise Tunnel" der Rhätischen Bahn. Geomechanik Und Tunnelbau 10 (5), 542–550. https://doi.org/10.1002/geot.201700029.

Guan, W., & Cheng, X. (2023). In-situ experimental study on heat exchange capacity of long-span energy tunnel exchangers. *Symp. Energy Geotech. 2023*, *October*, 59490. https://doi.org/10.59490/seg.2023.545.

Insana, A., Barla, M., 2020. Experimental and numerical investigations on the energy performance of a thermo-active tunnel. Renew. Energy 152, 781–792. https://doi.org/10.1016/j.renene.2020.01.086.

Insana, A., Barla, M., Sulem, J., 2020. Energy tunnel linings thermo-mechanical performance: Comparison between field observations and numerical modelling. E3S Web of Conferences 205. https://doi.org/10.1051/e3sconf/202020506008.

Johnsson, J., Adl-Zarrabi, B., 2019. Modeling the thermal performance of low temperature hydronic heated pavements. Cold Reg. Sci. Technol. 161 (February), 81–90. https://doi.org/10.1016/j.coldregions.2019.03.007.

Johnsson, J., & Adl-Zarrabi, B. (2020). A numerical and experimental study of a pavement solar collector for the northern hemisphere. *Appl. Energy*, *260*(June 2019), 114286. https://doi.org/10.1016/j.apenergy.2019.114286.

Kong, G., Wu, D., Wei, Y., 2023. Experimental and numerical investigations on the energy and structural performance of a full-scale energy utility tunnel. Tunn. Undergr. Space Technol. 139 (May). https://doi.org/10.1016/j.tust.2023.105208.

Laloui, L., Di Donna, A., 2013. *Energy geostructures: innovation in underground engineering*. John Wiley & Sons.

Lee, C., Park, S., Won, J., Jeoung, J., Sohn, B., Choi, H., 2012. Evaluation of thermal performance of energy textile installed in Tunnel. Renew. Energy 42, 11–22. https://doi.org/10.1016/j.renene.2011.09.031.

Lee, C., Park, S., Choi, H.J., Lee, I.M., Choi, H., 2016. Development of energy textile to use geothermal energy in tunnels. Tunn. Undergr. Space Technol. 59, 105–113. https://doi.org/10.1016/j.tust.2016.06.014.

Ma, C., Di Donna, A., Dias, D., Zhang, T., 2021a. Thermo-hydraulic and sensitivity analyses on the thermal performance of energy tunnels. Energ. Buildings 249, 111206. https://doi.org/10.1016/j.enbuild.2021.111206.

Ma, C., Donna, A.D., Dias, D., Zhang, J., 2021b. Numerical investigations of the tunnel environment effect on the performance of energy tunnels. Renew. Energy 172, 1279–1292. https://doi.org/10.1016/j.renene.2021.03.104.

Ma, C., Di Donna, A., Dias, D., 2022. Numerical study on the thermo-hydro-mechanical behaviour of an energy tunnel in a coarse soil. Comput. Geotech. 151 (August), 105003. https://doi.org/10.1016/j.compgeo.2022.105003.

Mazzola, M., Giordano, M., Alessio, C., Spigarelli, B., 2023. Autostrade per l'Italia (ASPI) TRS Tunnel Renewal Strategy: the cases of Castello 1 left, San Fermo right and Colle Marino left tunnels. Expanding Underground - Knowledge and Passion to Make a Positive Impact on the World- Proceedings of the ITA-AITES World Tunnel Congress, WTC 2023, 126–134. https://doi.org/10.1201/9781003348030-16.

Meibodi, S.S., Loveridge, F., 2022. The future role of energy geostructures in fifth generation district heating and cooling networks. Energy 240, 122481. https://doi.org/10.1016/j.energy.2021.122481.

Mirzanamadi, R., Hagentoft, C.E., Johansson, P., 2018a. An analysis of hydronic heating pavement to optimize the required energy for anti-icing. Appl. Therm. Eng. 144 (August), 278–290. https://doi.org/10.1016/j.applthermaleng.2018.08.053.

Mirzanamadi, R., Hagentoft, C.E., Johansson, P., 2018b. Numerical investigation of harvesting solar energy and anti-icing road surfaces using a hydronic heating

pavement and borehole thermal energy storage. Energies 11 (12), 1–23. https://doi.org/10.3390/en11123443.

Mirzanamadi, R., Hagentoft, C.-E., & Johansson, P. (2019). Numerical Investigation of Anti-Icing Road Surfaces using Hydronic Heating Pavement- Parametric Study. *16th IBPSA International Conference and Exhibition*, *2008*, 524–531. https://doi.org/10.26868/25222708.2019.211126.

Nicholson, D.P., Chen, Q., De Silva, M., Winter, A., Winterling, R., 2014. The design of thermal tunnel energy segments for Crossrail, UK. Proc. Inst. Civ. Eng. Eng. Sustainability 167 (3), 118–134. https://doi.org/10.1680/ensu.13.00014.

Ogunleye, O., Singh, R. M., & Cecinato, F. (2021). Assessing the thermal efficiency of energy tunnels using numerical methods and Taguchi statistical approach. *Appl. Thermal Eng.*, *185*(November 2020), 116377. https://doi.org/10.1016/j.applthermaleng.2020.116377.

Panebianco, A. (2023). *L'assessment gallerie alla luce delle recenti linee guida - prime applicazioni e risvolti progettuali.*

Peltier, M., Rotta Loria, A. F., Lepage, L., Garin, E., & Laloui, L. (2019). Numerical investigation of the convection heat transfer driven by airflows in underground tunnels. *Appl. Thermal Eng.*, *159*(November 2018), 113844. https://doi.org/10.1016/j.applthermaleng.2019.113844.

Pigorini, A. (2020). *Tunnelling 4.0: New technologies and future perspectives for maintenance, refurbishment interventions and upgrading.* https://beyondatunnelvision.eu/programme/parallel-sessions.

Rotta Loria, A.F., 2021. The thermal energy storage potential of underground tunnels used as heat exchangers. Renew. Energy 176, 214–227. https://doi.org/10.1016/j.renene.2021.05.076.

Rotta Loria, A.F., Di Donna, A., Zhang, M., 2022. Stresses and deformations induced by geothermal operations of energy tunnels. Tunn. Undergr. Space Technol. 124 (March), 104438. https://doi.org/10.1016/j.tust.2022.104438.

Salciarini, D., Gerola, M., De Feudis, S., Lupattelli, A., Dalla Santa, G., Capati, G., Rafai, M., Tihana, J., Scerbo, M., Donna, A. Di, Ravera, E., Nicolino, M., Insana, A., Mroueh, H., & Barla, M. (2026). Database-driven analysis of energy geostructures using a global dataset : Diffusion, efficiency, and environmental performance. *Renew. Energy*, *256*(Part F), 124373. https://doi.org/10.1016/j.renene.2025.124373.

Sethi, R., Casasso, A., Piga, B., & Ruffino, E. (2021). Il potenziale geotermico a bassa entalpia nella Regione Piemonte. Technical report, Politecnico di Torino.

Seywald, C., Helmberger, A., Matt, R., 2017. Innovative Methode zur Ertüchtigung alter Eisenbahntunnel unter Betrieb – Beispiel Rekawinkler- und Kleiner Dürrebergtunnel. Geomechanik Und Tunnelbau 10 (5), 533–541. https://doi.org/10.1002/geot.201700030.

Unterberger, W., Hofinger, H., Grünstäudl, T., Adam, D., Markiewics, R., 2004. Utilization of Tunnels as sources of Ground Heat and Cooling–Practical applications in Austria. In: *Proceedings of the ISRM International Symposium 3rd ARMS*, pp. 421–426.

Zhang, G., Xia, C., Yang, Y., Sun, M., Zou, Y., 2014. Experimental study on the thermal performance of tunnel lining ground heat exchangers. Energ. Build. 77, 149–157. https://doi.org/10.1016/j.enbuild.2014.03.043.

Zhou, B., Pei, J., Richard Hughes, B., SNM Nasir, D., Vital, B., Pantua, C.A.J., Calautit, J., Zhang, J., 2021. Structural response analysis of road pavement solar collector (RPSC) with serpentine heat pipes under validated temperature field. Construct. Build. Mater. 268, 121110. https://doi.org/10.1016/j.conbuildmat.2020.121110.